

Temporal Action Segmentation: An Analysis of Modern Techniques

Guodong Ding*, Fadime Sener*, and Angela Yao

Abstract—Temporal action segmentation (TAS) from videos aims at densely identifying video frames in minutes-long videos with multiple action classes. As a long-range video understanding task, researchers have developed an extended collection of methods and examined their performance using various benchmarks. Despite the rapid growth of TAS techniques in recent years, no systematic survey has been conducted in these sectors. In this survey, we analyze and summarize the most significant contributions and trends to this endeavor. In particular, we first examine the task definition, common benchmarks, types of supervision, and prevalent evaluation measures. In addition, we systematically investigate two essential techniques of this topic, *i.e.*, frame representation, and temporal modeling, which have been studied extensively in the literature. We then conduct a thorough review of existing TAS works categorized by their levels of supervision and conclude our survey by identifying and emphasizing several research gaps. In addition, we have curated a list of TAS resources, which is available at <https://github.com/atlas-eccv22/awesome-temporal-action-segmentation>.

Index Terms—Temporal Action Segmentation, Video Representation, Temporal & Sequential Modeling, Literature Survey

arXiv:2210.10352v3 [cs.CV] 3 Mar 2023

1 INTRODUCTION

TEMPORAL action segmentation (TAS) is a video understanding task that segments in time a temporally untrimmed video sequence. Each segment is labeled with one of a finite set of pre-defined action labels (see Fig. 1 for a visual illustration). This task is a 1D temporal analogue to the more established semantic segmentation [1], replacing pixel-wise semantic labels to frame-wise action labels. Automatically segmenting untrimmed video sequences helps to understand what actions are being performed, when they started, how far they have progressed, what type of transformations are brought to the environment through these actions, and what people will do next. It also enables diverse downstream applications, such as video security or surveillance systems, assistive technologies, and human-robot interactions. This survey first introduces the techniques required to understand the task, followed by a comprehensive overview of recent TAS methods.

In computer vision, *action recognition* is the hallmark task for video understanding. In action recognition, pre-trimmed video clips of a few seconds are classified with single semantic labels. State-of-the-art methods [2], [3], [4] can distinguish hundreds of classes. However, classifying pre-trimmed clips is a highly limiting case as the video feeds of surveillance systems, autonomous vehicles, and other real-world systems occur in streams. The individual actions or events are related and may span well beyond a few seconds. As a result, standard action recognition approaches are not directly applicable.

TAS methods target untrimmed video sequences as opposed to action recognition on pre-trimmed video clips. The

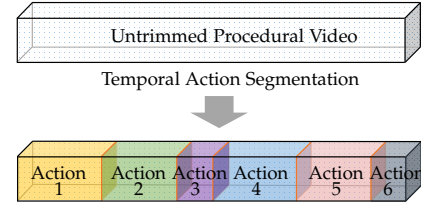


Fig. 1: A TAS model segments an untrimmed video sequence in the temporal dimension into successive actions.

videos portray a series of multiple actions, which typically span several minutes. A common “*making coffee*” procedural video may include the following steps: ‘take cup’, ‘pour coffee’, ‘pour sugar’, ‘pour milk’, and ‘stir coffee’. In the domain of procedural videos, the prevalent word for the overall procedure is *(complex) activity*, whereas the composing steps are *actions*. Importantly, the steps often adhere to a loose temporal ordering, *i.e.*, permutations of some actions in time (‘pour coffee’ and ‘pour milk’), or the lack of certain actions (‘pour sugar’) still accomplishes the goal.

An effective TAS model must be able to utilize sequential information to appropriately determine action boundaries. This leads to two considerations: frame-level representations that are discriminative and long-range temporal modeling. Frame-level representations should capture both static and dynamic visual information for discrimination. Furthermore, the sequential dynamics of actions should be well captured. The ordering characteristics of actions raise a fundamental question - how should temporal or sequential relationships be modeled to account for action repetition, duration, and order variations? Therefore, this survey identifies the aforementioned two aspects as the essential techniques for the TAS task and provides respective in-depth analyses.

Contributions: There are several surveys on human

• Guodong Ding and Angela Yao are with the School of Computing, National University of Singapore, Singapore (emails: dinggd@comp.nus.edu.sg, ayao@comp.nus.edu.sg).
 • Fadime Sener is a research scientist at Meta Reality Labs (email: fadimesener@meta.com).
 • * indicates equal contribution.

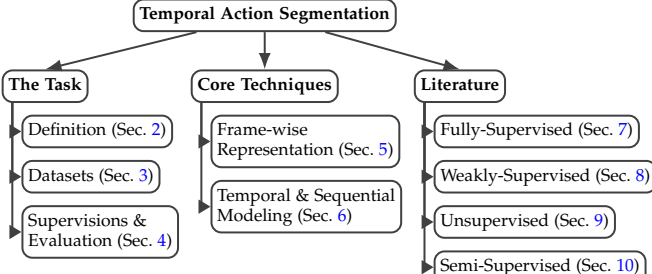


Fig. 2: The taxonomy of existing temporal action segmentation research.

activity understanding in videos, though their focus is primarily on action recognition [5], [6], temporal action localization [7], [8], action anticipation [9], [10], *etc.* To the best of our knowledge, this is the first survey to provide a thorough overview of TAS works. In addition to categorizing existing works, we propose a taxonomy that emphasizes their contributions.

Additionally, we compare the existing datasets by analyzing their characteristics. In doing so, we present two metrics, *i.e.*, repetition and order variation scores, which characterize the temporal dynamics of actions and demonstrate that the majority of these datasets are limited in action repetition and order variation. We further distinguish several performance evaluation and comparison settings. We provide a standardized evaluation setup for unsupervised segmentation methods and a class-based evaluation metric emphasizing the long-tail distribution. Lastly, we present a handful of intriguing future areas and problems for the community to investigate.

1.1 Survey Structure

Fig. 2 outlines a taxonomy of the TAS task and the structure of this survey. Section 2 provides a formal task description and compares it with other related tasks. Sections 3 and 4 compares the benchmarks, forms of supervision, evaluation metrics and settings, respectively. Section 5 delves into how frames are embedded and embellished, summarizing the widespread usage of handcrafted models or deep learning backbones for feature extraction. Section 6 outlines the temporal and sequential modeling techniques employed in TAS. Sections 7 to 10 provides a comprehensively curated list of TAS approaches grouped according to the type of supervision. Finally, Section 11 concludes the survey by discussing challenges and future research directions.

2 TEMPORAL ACTION SEGMENTATION

2.1 Task Description

Temporal action segmentation aims to segment a temporally untrimmed video by time and label each segmented part with a pre-defined action label [11]. Formally, given a video $x = (x_1, x_2, \dots, x_T)$ of length T with N actions, TAS methods produce the following output:

$$s_{1:N} = (s_1, s_2, \dots, s_N) \quad (1)$$

where $s_n = (c_n, \ell_n)$ represents a continuous video segment of length ℓ_n that has the semantic label c_n out of \mathcal{C} pre-defined categories. The task can also be regarded as a 1D

TABLE 1: TAS has its own unique position in the task landscape, differentiating the tasks based on whether they involve Temporal Relation between action instances in videos, Boundary Localization of actions, Segment Semantic understanding, and the Data Domain.

Task	Temporal Relation	Boundary Localization	Segment Semantic	Data Domain
TAS	✓	✓	✓	video
TAD/L	✗	✓	✓	video
SS	✓	✓	✓	audio, motion
KFD	✓	✗	✓	video, text
CAC	✓	✗	✗	video
GEBD	✗	✓	✗	video

version of semantic (image) segmentation, and can analogously be formulated as a frame-wise action classification, *i.e.*,

$$y_{1:T} = (y_1, y_2, \dots, y_T) \quad (2)$$

where y_t is the action label of frame t . The segment formulation is commonly used in works that predict the most probable sequence of actions [12], [13], while the latter, frame-wise formulation is popular with deep learning-based methods [14]. The two formulations, however, are equivalent and one can easily reconstruct one from the other.

2.2 Related Tasks

There are several tasks in video understanding which are closely related to TAS. They can be distinguished with TAS based on their data domain, identification of segment semantics as well as the reasoning of temporal dynamics between segments. The related tasks are described below and compared in Tab. 1.

Temporal Action Detection / Localization (TAD/L) [15], [16] detects the start and end of action instances and predicts semantic labels simultaneously. TAD/L works more with general videos that allow overlap in the actions while TAS works with procedural videos to find a change point between actions.

Sequence Segmentation (SS) is popular in other domains, including motion capture data [17], [18], [19] and audio signals [20]. Most approaches are developed to segment individual sequences [17], [18], [19] while some [21] focuses on multiple motion capture recordings simultaneously. However, such data is lower-dimensional and exhibits much less variance than video.

Key-Frame Detection (KFD) identifies single characteristic frames or key-steps [22], [23], [24], [25] for actions. Like TAS, KFD requires modeling the temporal relations between actions; however, it is out of the task scope to find the boundary where the actions transition.

Complex Activity Classification (CAC) [37], [38] targets classifying the complex activity of procedural videos. Such a task is similar to TAS in the way it models the temporal relations of actions. Still, it is not concerned with the individual frames as CAC is aimed to determine the complex activity class of the full action sequence.

Generic Event Boundary Detection (GEBD) [39] localizes the moments where human perceive as event boundaries. The boundaries signify changes in action, subject, and environment. In comparison, GEBD does not work with

TABLE 2: Comparisons of procedural activity datasets in a chronological order. The first group of datasets are Recorded while the second group of datasets are from Online media platforms, *e.g.*, YouTube. We report the Duration, the number of videos (# Videos), segments (# Segments), procedural activities (# Activity), actions (# Action) and Domain for each dataset. The View of datasets might be Egocentric, 3rd Person, Top-view, or Mixed.

	Dataset	Year	Duration	# Videos	# Segments	# Activity	# Action	Domain	View
Recorded	[26] GTEA	2011	0.4h	28	0.5K	7	71	Cooking	Egocentric
	[27] 50Salads	2013	5.5h	50	0.9K	1	17	Cooking	Top-view
	[28] Breakfast	2014	77h	1712	11K	10	48	Cooking	3rd Person
	[29] Epic-Kitchens	2020	200h	700	90K	-	4053	Daily	Egocentric
	[30] Ikea ASM	2021	35h	371	16K	4	33	Furniture	3rd Person
	[31] Meccano	2021	0.3h	20	8.9K	1	61	Assembly	Egocentric
	[32] Assembly101	2022	513h	4321	1M	15	202	Assembly	Egocentric + 3rd Person
	[33] HA4M	2022	6h	217	4.1K	1	12	Manufacture	3rd Person
Online	[34] YouTube Instructional	2016	7h	150	-	5	47	Mixed	Mixed
	[35] YouCookII	2018	176h	2K	15K	89	-	Cooking	Mixed
	[22] CrossTask	2019	376h	4.7K	34K	83	107	Mixed	Mixed
	[36] COIN	2019	476h	11.8K	46K	180	778	Mixed	Mixed

semantic labels nor assume any temporal relations between detected boundaries.

3 DATASETS

3.1 Core Datasets

Datasets used for TAS usually feature procedural activities. Actors execute a sequence of actions, with some order, to arrive at a goal, such as making a dish, or assembling some furniture. Such datasets are annotated with action segments' start and end boundaries and action labels. Four datasets used in TAS works are described as follows.

GTEA [26] contains 28 videos of seven procedural activities recorded in a single kitchen. The videos are recorded with a camera mounted on a cap worn by four participants.

50Salads [27] is composed of 50 recorded videos of 25 participants making two different mixed salads. The videos are captured by a camera with a top-down view of the work surface. The participants are provided with recipe steps, which are randomly sampled from a statistical recipe model.

Breakfast Actions [28] targets recording videos “in the wild”, in 18 different kitchens, as opposed to the controlled lab environments in the previous datasets [26], [27]. The dataset features 52 participants performing ten breakfast-related activities and is recorded with 3 to 5 cameras, all from the third-person point of view.

YouTube Instructional [34] is a collected dataset and includes five instructional activities. There are 30 videos for each activity. This dataset is mainly used for unsupervised segmentation.

Assembly101 [32] is a collected dataset where 53 participants are asked to disassemble and assemble take-apart toys without being given any instructions. The dataset is annotated with fine-grained, hand-object interactions and coarse action labels. The authors evaluate their dataset for TAS using coarse labels.

3.2 Related Datasets

There are several other long-range procedural activity datasets. In this section, we present these datasets and explain why it is challenging or not preferable to explore temporal segmentation on these datasets.

Epic-Kitchens [40] is a large-scale egocentric dataset with 100 hours of recording. Videos last 1 - 55 minutes.

Although it comprises long-range videos, its overlapping segments and fine-grained action labels may make it unsuitable for segmentation.

Ikea ASM [30] includes videos of the assembly of four types of IKEA furniture and annotates fine-grained actions.

Meccano [31] is a recorded dataset of 20 people assembling a toy motorbike featuring only fine-grained actions.

HA4M [33] documents 41 subjects constructing an epicyclic gear train with 12 actions by multi-modal data sensors. Despite the absence of TAS benchmarks on this dataset, it remains a viable option for TAS.

YouCookII [35] is collected from YouTube. Each video, all from cooking recipes, is annotated with the temporal boundaries of the recipe steps and their textual description, but no action labels are to be used in the TAS works.

CrossTask [22] is a YouTube collection of 18 primary tasks with temporal location annotations and 65 related tasks without any temporal annotations. CrossTask is used to assess unsupervised segmentation algorithms, but not supervised or weakly supervised ones.

COIN [36] is a dataset from YouTube with 180 diverse tasks from twelve domains. The typical video has four segments, making sequence dynamics less interesting.

3.3 Dataset Comparison & Discussion

Tab. 2 makes a detailed comparison of the procedural video datasets. The datasets are divided according to their source, scale, number of actions, and viewpoint, either recorded or collected from online platforms.

Recorded datasets have either third-person or egocentric views. Datasets with third-person view only contain constrained backgrounds and focus more on foreground action. However, they may suffer from the occlusions of actions due to the fixed view of cameras. While the egocentric view is better at capturing objects and tools to recognize the hand object interactions, the camera motion poses extra challenges to action recognition. The Epic-Kitchens dataset [29] is the largest egocentric vision dataset capturing untrimmed daily activities. There are also several procedural activity datasets with an egocentric view, *e.g.*, [26], [41], but on a much smaller scale. Breakfast [28] contains recordings with multiple third-person views. Only Assembly101 [32] provides both egocentric and third-person views.

Sourcing videos from online platforms is a convenient way to build up large-scale and varied datasets [22], [35],

TABLE 3: Temporal dynamics of coarse action segments. A higher value in **Repetition** score indicates more action repetition, while a lower value in **Order Variation** score indicates looser action ordering constraints.

Dataset	Repetition $r \uparrow$	Order Variation $v \downarrow$
[27] 50Salads	0.08	0.02
[28] Breakfast	0.11	0.15
[32] Assembly101	0.18	0.05

[36], [42], [43]. Such datasets are useful for training offline retrieval systems, but may not be applicable for real-time scenarios as the videos are edited, *e.g.*, with fast-forwarding, annotated frames or changing viewpoints.

Given the increasing number of "how to" videos, procedural activity understanding is a particularly interesting topic for research. Moreover, it can have a significant impact on real-time intelligent systems that assist with various tasks. Yet, the diversity of existing activity datasets is rather limited. With a few recent exceptions [30], [31] almost all the recorded datasets cover only cooking activities. These datasets are too small. As of the moment, Assembly101 [32] is the only dataset that offers a large-scale data which is beyond the kitchen domain.

3.4 Background Frames

Some videos feature task-irrelevant segments. For example, the actor may introduce tools or perform alternative ways to complete an action, etc. Such ‘background frames’ occur at arbitrary locations with varying lengths, and are common in datasets collected from YouTube, such as YouTube Instructional [34], YouCookII [35], and CrossTask [22]. In most existing TAS works, the background class is treated equivalently to other action classes and used for training and evaluation.

3.5 Temporal Dynamics

A defining characteristic of the TAS task is the sequential relationship between the actions. To better understand and characterize the sequence dynamics, we propose a repetition score and an order variation score and compare the core datasets according to these scores in Tab. 3.

The **repetition score** r reflects the extent of repeated actions, and is formulated as,

$$r = 1 - u/g \quad (3)$$

where u is the number of unique actions in one video instance, g is the total number of actions, and r is a score that falls in the range of $[0, 1]$. 0 indicates no repetition, and the closer the score is to 1, the more repetition occurs in the sequence.

The **order variation score** v is defined as the normalized average edit distance, $e(R, G)$, between every pair of sequences, (R, G) . It is then normalized with respect to the maximum sequence length of the two,

$$v = 1 - e(R, G) / \max(|R|, |G|) \quad (4)$$

This score has a range of $[0, 1]$; 1 corresponds to no deviations in ordering between pairs. Scores close to 1 indicate that actions follow a strict ordering, making it less necessary

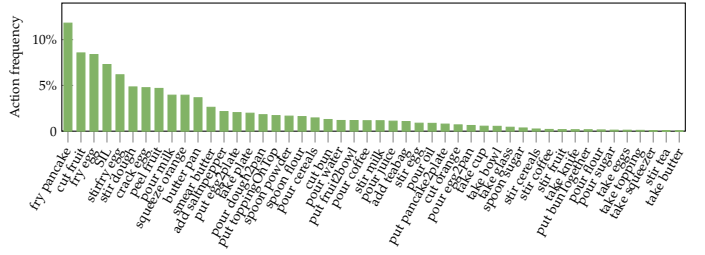


Fig. 3: Action frequency on Breakfast [28], sorted by descending order. ‘SIL’ indicates the ‘background’ where no action of interest occurs. The head class ‘fry pancake’ is $639 \times$ more frequent than the tail class ‘take butter’.

TABLE 4: Imbalance Ratio (IR) on four TAS datasets.

Dataset	GTEA	50Salads	Breakfast	Assembly101
IR	24	6	639	2604

to model temporal sequence dynamics. On the other hand, a lower score, like in 50Salads, indicates the highest amount of ordering variations as salad items can be added in any order, making modeling the temporal relations between actions less beneficial.

Assembly101 positions itself as a challenging and interacting benchmark for modeling the sequence relations between actions. As indicated in Tab. 3, Assembly101’s order variation score sits between Breakfast and 50Salads, and includes $1.6\times$ and $2.3\times$ more repeated steps than the two datasets respectively.

3.6 Action Frequency

The long-tailed action frequency is an overlooked aspect of per-frame classification formulation (Eq. (2)) of TAS. In procedural videos, it is natural that some actions require a longer time to perform than others, *e.g.*, ‘fry egg’ is considerably more time-consuming than ‘crack egg’. We calculate the action frequency as the proportion each action label takes in the whole dataset, *i.e.*, $n_c / \sum_{i=1}^C n_i$, where n_c is the number of frames with label c . Fig. 3 illustrates the action frequency on Breakfast [26], which depicts the imbalanced frequencies across actions.

A commonly adopted value to indicate the skewness of the action distribution is the imbalance ratio (IR) [44], [45]. IR is defined as the ratio between the number of frames in the head and the tail classes (n_1/n_K) sorted by the decreasing order of cardinality (*i.e.*, if $i_1 > i_2$, then $n_{i_1} \geq n_{i_2}$ and $n_1 \gg n_K$). Tab. 4 shows that 50Salads [27] has the smallest IR value of 6, marking a less imbalanced scenario between actions; while, Assembly101 [32] is highly skewed in action frequencies with an IR of 2604. Such a long-tailed nature of the datasets poses extra challenges to the TAS task.

4 SUPERVISION AND EVALUATION

4.1 Task Supervision

Like many other computer vision tasks, TAS has been investigated under different forms of supervisions. Tab. 5 lists the forms of supervision in descending order in terms of annotation effort, *i.e.*, from fully supervised to unsupervised.

TABLE 5: Comparison of supervisory signals and evaluation prerequisites in TAS. Full, semi-supervision, and single-frame under weak supervision provide labels for video frames, and their performance is directly evaluated on model outputs without any pre-steps. Action lists or set supervision do not provide exemplars and their evaluation is based on the best-matched action list filtered with maximum sequence posterior per test video. Activity label setting uses video-level labels all at once while unsupervised uses them one at a time. Hungarian matching is required for both before evaluation.

Full (Section 7)		Semi (Section 10)	Weak (Section 8)			Unsupervised (Section 9)
			Single-frame	Action List/Set	Activity Label	
Action-level	Dense frame-wise	subset with Dense frame-wise	Ordered list + Exemplar frames	(Ordered) list, Union set	-	-
Video-level	-	-	-	-	All activities <i>en masse</i>	One activity at a time
Evaluation prerequisite	-	-	-	Maximum Sequence Posterior (Section 4.3)	Hungarian Matching (Section 4.4)	Hungarian Matching (Section 4.4)

A fully-supervised setting provides dense action labels for every frame in training video sequences [14], [46]. Dense labels are the most time-consuming to collect per video sequence as it requires the annotator to view the entire video sequence. A semi-supervised [47], [48] setting reduces the annotation effort proportionally by annotating a subset of the videos densely while treating the remaining videos as unlabeled samples.

Weak labels require less annotation effort than dense video labels. Weak labels from the literature include single-frames [49], [50], action lists or action sets [12], [13], and activity labels [51]. Single-frames, or time-stamp annotations, are sparsely labeled frames, and can be viewed as an ordered list of actions associated with exemplar frames. Removal of the exemplar frames would form an action list, which is also referred to as the action transcript. Further reducing the ordering of actions, and repetitive entries from the action list leads to the even weaker action set. The above-listed weak labels are all based on action-level annotations. Recently, video-level complex activity labels [51] are used to supervise the TAS task, which is the weakest supervision because no action level information is provided.

The unsupervised setting in TAS in previous works [52], [53], [54] considers collections of videos that perform the *same* activity. In this regard, it is not label-free, as it requires the activity label to form the video collections. The unsupervised setting then is comparable with the weak activity label supervision in terms of label information. However, the two settings differ in how the collections of videos are processed during training. Formally, unsupervised works work with one group of the same activity videos at a time, while activity label supervision works with videos from all activities simultaneously.

4.2 Evaluation Measures

Three commonly adopted evaluation metrics in TAS are Mean of Frames (MoF), Edit Score, and F1-scores. The first is a frame-based measure (see Section 4.2.1), while the latter two are segment-based measures (see Section 4.2.2). All three metrics are used in full, weak, and semi-supervised settings. For unsupervised settings, only F1 and MoF are reported in the literature. By definition, the evaluation of the unsupervised works is conditioned on the association between clusters and semantic labels. The Hungarian matching algorithm has been adopted to enable the evaluation by mapping learned frame clusters to semantic labels, which we elaborate in detail in Section 4.4.

4.2.1 Frame-Based Measures

Mean over Frames (MoF), also referred to as frame-wise Accuracy (Acc), is defined as the fraction of the model's correctly predicted frames:

$$\text{MoF} = \frac{\text{\# of correct frames}}{\text{\# of all frames}}. \quad (5)$$

The Acc metric is problematic when the action frame distribution is imbalanced. This is true for most datasets, as dominating (long) actions class can have a strong impact on the value. The existence of such imbalance as we have discussed in Section 3.6 makes this more likely to happen. This also implies that models achieving similar accuracy may have large qualitative differences. Therefore, a class-averaged accuracy metric would help better interpret the model performance, e.g.,

$$\text{mMoF} = \sum_c \text{MoF}(c)/|\mathcal{C}| \quad (6)$$

where $\text{MoF}(c)$ is the frame accuracy per class c .

Another drawback of MoF is that its per-frame calculation can not reflect the segmental quality. The MoF score could be high even when the segmentation results are fragmented. Such division of a durative action into many discontinuous sub-segments is referred to as over-segmentation. However, over-segmentation can be evaluated by segment-based measures, as introduced next.

4.2.2 Segment-Based Measures

The segment-based F1-score [46] and Edit Score [55] are evaluation metrics that more focus on the segment errors.

The F1-score or $\text{F1}@\tau$ [46] compares the Intersection over Union (IoU) of each segment with respect to the corresponding ground truth based on some threshold $\tau/100$. A segment is considered a true positive if its score with respect to the ground truth exceeds the threshold. If there is more than one correct segment within the span of a single ground truth action, then only one is considered a true positive and the others are marked as false positives. Based on the true and false positives as well as false negatives (missed segments), one can compute the precision and recall and blend the two into the harmonic mean to get

$$\text{F1} = 2 \cdot \frac{\text{precision} * \text{recall}}{\text{precision} + \text{recall}}. \quad (7)$$

Normally, τ values are set to $\{10, 25, 50\}$.

The Edit Score [55] quantifies the similarity of two sequences. It is based on the Levenshtein distance and

tallies the minimum number of insertions, deletions, and replacement operations required to convert one segment sequence into another. By denoting by X and Y the ordered list of predicted and ground truth action segments, the accumulative distance value e is defined as:

$$e[i, j] = \begin{cases} \max(i, j), & \min(i, j) = 0 \\ \min(e[i-1, j] + 1, e[i, j-1] + 1, \\ e[i-1, j-1] + \mathbb{1}(X_i = Y_j)), & \text{otherwise.} \end{cases} \quad (8)$$

where $i \in |X|, j \in |Y|$ are indices for X and Y , respectively, and $\mathbb{1}(\cdot)$ is the indicator function. The above problem can be effectively solved by dynamic programming. The Edit Score is then normalized by the maximum length of the two sequences and is computed as:

$$\text{Edit} = \frac{1 - e(X, Y)}{\max(|X|, |Y|)} \cdot 100. \quad (9)$$

This metric measures how well a model predicts the action segment ordering without requiring exact frame-wise correspondence to the ground truth.

Given a TAS model that outputs frame-wise action probability scores, its performance is directly evaluated by taking frame-wise predictions and comparing them with their corresponding ground truth labels to compute the three scores defined above.

4.3 Weakly-Supervised Evaluation

For the model inference on the test set where no reference action list or set is available, Richard *et. al.* [13] presumes that the set of actions appearing in a test video overlaps with that from the training set, *i.e.*, there is at least one training video sharing the same ground truth action set as the test video. Similarly, Li and Todorovic [56] follow [13] and use Monte Carlo sampling of potential action sequences but discard candidate sequences that do not include all actions in that video. Out of all K sampled candidates, the action sequence that gives the maximum posterior modeled by a Hidden Markov Model (HMM) Eq. (15) is selected as the final solution. A detailed description of the posterior estimation is provided in Section 6.2.1.

4.4 Unsupervised Evaluation

Without some correlation between the estimated agnostic segments and ground truth actions, the evaluation metrics in Section 4.2 are not directly applicable to the unsupervised scenario. The Hungarian matching algorithm [57] is a combinatorial algorithm used to find maximum-weight matching in bipartite graphs, and it has been widely utilized for evaluating unsupervised clustering tasks [58], [59].

In unsupervised TAS, Hungarian matching links the given frames X of N clusters to the action label corpus Y of M classes by finding the best matching $\hat{\mathcal{A}} \subset \{0, 1\}^{N \times M}$:

$$\begin{aligned} \hat{\mathcal{A}} = \arg \max_{\mathcal{A}} \sum_{n,m} \mathcal{A}_{n,m} \cdot I(X_n, Y_m), \\ \text{s.t. } |\mathcal{A}| = \min(N, M) \end{aligned} \quad (10)$$

where X_n denotes frames belonging to cluster n , and Y_m denotes frames with the action label m . $\mathcal{A}_{n,m}$ is the indicator

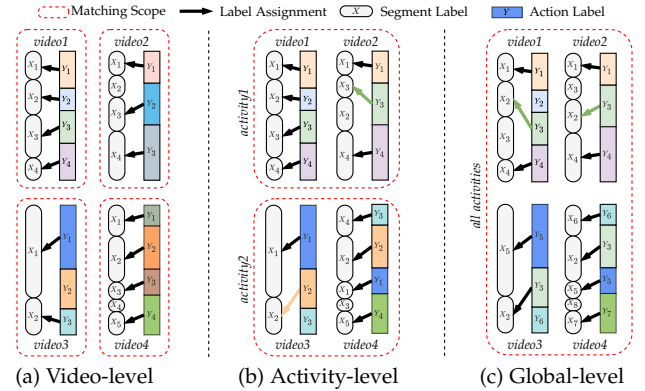


Fig. 4: Four videos from two complex activities with varying Hungarian matching levels. Colored rectangles denote ground truth actions, while rounded rectangles denote video segments. Hungarian matching scopes are red dashed rectangles. Black dashed arrows indicate matched segments, while the coloured arrows highlight changed matching across levels. With scope changing from the video (a) to activity (b), change in GT Y across different videos results in the change of label association for $video2$ (green) and $video3$ (orange). A similar change of assignments happens when the matching is done on the global level (c). Unmatched segments (X_2 in $video2$ at video-level matching (a)) are considered as background.

function for assigned pair (n, m) , $I(X_n, Y_m)$ is the number of frames with ground-truth class label m that appear in cluster n . When two parties have equivalent classes ($N=M$), the Hungarian matching constructs a bijection. Otherwise, it produces a one-sided perfect matching of size $\min(N, M)$. The remaining mismatched clusters are treated as background automatically. The evaluations are then based on the corresponding results.

Depending on the bipartite set's scope, Hungarian matching can be applied at three different levels, as illustrated in Fig. 4.

Video-level matching [53], [60] matches the cluster with respect to the ground truth actions of a *single* video. This matching evaluates the ability of a model to segment a video sequence into distinct actions. This matching produces the best performance given it is done per video. In Fig. 4(a), within each matching scope, the Hungarian matching is agnostic of the possible association of actions across videos.

Activity-level matching associates clusters to labels within each complex activity. Most unsupervised works [52], [61], [62] follow this level of matching, *i.e.*, process videos from the same activity. As shown in Fig. 4(b), the activity level of grouping leads to the assignment changes denoted by colored arrows.

Lastly, **global-level** matching is performed on the entire dataset. This is the most challenging setting as both intra- and inter-activity matching must be considered. It is noteworthy that [61] report different 'global' matching results across complex activities, as their setting does not consider actions shared across complex activities.

The various scopes of Hungarian matching correlate to distinct learning objectives of a TAS model; the greater the scope, the more difficult the task. Video-level matching simply sets the requirement of differentiating actions within a video, *i.e.*, *intra-video action discrimination*. For activity-

TABLE 6: Comparison between model learning requirements in different levels of Hungarian matching for action segmentation. For **video-level** matching, Intra-Video Discrimination of actions is sufficient. To enable an **activity-level** matching, the model needs to take into consideration Intra-Activity Association. Meanwhile, the **global-level** matching sets the highest learning requirement with additional Inter-Activity Association between actions.

Matching Level	Intra-Video Discrimination	Inter-Activity Association	Inter-Activity Association
Video	✓	✗	✗
Activity	✓	✓	✗
Global	✓	✓	✓

level matching, a model must discriminate between actions within a video and also acquire extra *intra-activity action association* knowledge. In the global-level matching, a model must additionally include *inter-activity associations* to construct feasible action correspondences across complex activities. The differences between these learning requirements are summarized in Tab. 6. Note that a model learned at a broader scope is **downward compatible** and can be adjusted to be evaluated at a finer scope, *e.g.* from global to activity level, but not vice-versa. Despite the practical feasibility of doing so, the results cannot be directly compared due to the models' disparate learning requirements.

5 FRAME-WISE REPRESENTATION

The standard practice in TAS is to use pre-computed frame-wise features (Section 5.1) as inputs due to the heavy computational demands of learning video features. Using pre-computed features has a key advantage in that it allows a dedicated comparison of the proposed architectures without the confounding influences of improved frame-wise feature representations. More recently, some works have aimed to make the pre-computed features more discriminative (Section 5.2) by embedding more task-specific knowledge.

5.1 Pre-Computed Features

5.1.1 Fisher Vector Encoded IDT

The original and Improved Dense Trajectories (IDT) [63], [64] were commonly used hand-crafted features for action recognition and video understanding before the rise of deep learning. The original dense trajectories features [63] are spatiotemporal features computed along tracks of interest points formed via optical flow. IDT [64] adds “improvements” by correcting the trajectories for camera motions. To apply IDT to action recognition, [64] further encode the raw trajectories by using Fisher Vectors (FV) [65] to capture the trajectories’ first and second-order statistics.

5.1.2 Inflated 3D ConvNet (I3D)

Inflated 3D ConvNet (I3D) [66] is a state-of-the-art architecture to extract generic features for video understanding. It uses as a backbone the pre-trained Inception-V1 [67] with 2D ConvNet inflation. In practice, it inflates all $N \times N$ spatial kernels to $N \times N \times N$ by replicating the original kernels N times and rescaling them with a temporal factor of $1/N$. The model is pre-trained on the Kinetics dataset [68] for action

recognition. Architecture-wise, the I3D model has two data streams *i.e.*, RGB and optical flow. The optical flow of the input video is computed by the TV-L1 algorithm [69]. Then, a $21 \times 224 \times 224$ spatiotemporal volume of RGB and flow frames are each fed into their respective branch to extract 1024D features. The two are then concatenated to compose the final 2048D representation [70].

5.2 Additional Feature Learning

5.2.1 Discriminative Clustering

To cluster the video features discriminatively, Sener *et al.* [52] first learn a linear mapping Φ of the input features $\mathbf{X} \in \mathbb{R}^V$ into a latent embedding space, *i.e.*, $\Phi(\mathbf{X}) \in \mathbb{R}^E$. In the latent space, they define a set of K anchors $\mathbf{W}_a \in \mathbb{R}^{K \times E}$ to represent the potential action classes. The latent feature descriptor is then defined as a similarity with respect to the anchors, denoted as $\mathbf{F} = \mathbf{W}_a^T \mathbf{W}_\Phi \mathbf{X}$, where $\mathbf{W}_\Phi \in \mathbb{R}^{E \times V}$ are the embedding weights of Φ . The learning objective for the latent space is defined as a pair-wise ranking loss:

$$L = \sum_t \sum_{k=1, k \neq k^*}^K \max[0, f_t^k - f_t^{k^*} + \Delta] + \gamma \|\mathbf{W}_a, \mathbf{W}_\Phi\|_2^2, \quad (11)$$

where f_t^k denotes the distance of f_t to an anchor k and k^* is the action label for that video frame. The term $\Delta > 0$ is a predefined parameter that ensures that f_t is closer in the latent space to its anchor k^* than other anchors by a margin. L_2 regularization is imposed on \mathbf{W}_a and \mathbf{W}_Φ , and γ is the weighting parameter. In an unsupervised setting, as the true action label is unknown, \mathbf{W}_a and \mathbf{W}_Φ are learned iteratively, and k^* is assigned based on the segmentation results from a previous step.

5.2.2 Contrastive Learning

Contrastive learning builds robust feature representations by contrasting samples against each other to learn attributes that are common between data classes and attributes that set a data class apart from the others [71], [72], [73]. Inspired by these works, Singhania *et al.* [47] apply contrastive learning to learn a set of stronger feature representations with a temporal encoder-decoder. The positive and negative sets of contrastive learning are selected based on clustering and temporal continuity.

The contrastive probability for a positive frame pair (i, j) from video (m, n) is defined as:

$$p_{i,j}^{nm} = \frac{e_\tau(f_i^n, f_j^m)}{e_\tau(f_i^n, f_j^m) + \sum_{(r,q) \in \mathcal{N}_{(n,i)}} e_\tau(f_i^n, f_r^q)}, \quad (12)$$

where e_τ is the exponential cosine similarity with temperature τ .

The complex activity label can provide further cues for contrastive learning. In [47], video-level features h_n for video n are formed by max-pooling the frame features along the temporal dimension, *i.e.* $h_n = \max_{1 \leq t \leq T_n} f_{(n,t)}$. For video n with activity c_n , video-wise positive and negative sets can be constructed from other videos of the same or different activities, *i.e.*, $\mathcal{P}_n = \{m : c_m = c_n\}$ and

$\mathcal{N}_n = \{m : c_m \neq c_n\}$ respectively. A contrastive probability for video n and its positive pair m is defined analogously as

$$p_{nm} = \frac{e_\tau(h_n, h_m)}{e_\tau(h_n, h_m) + \sum_{r \in \mathcal{N}_n} e_\tau(h_n, h_r)}. \quad (13)$$

Based on the frame- and video-level contrastive probabilities in Eq. (12) and Eq. (13), feature representations are learned with following contrastive loss:

$$\mathcal{L} = -\frac{1}{N_1} \sum_{n,i} \sum_{m,j \in \mathcal{P}_{n,i}} \log p_{ij}^{nm} - \frac{1}{N_2} \sum_n \sum_{m \in \mathcal{P}_n} \log p_{nm}, \quad (14)$$

where $N_1 = \sum_{n,i} |\mathcal{P}_{n,i}|$ and $N_2 = \sum_n |\mathcal{P}_n|$.

5.2.3 Temporal and Visual Embedding

For highly regular activities like those found in Breakfast Actions, the same action tends to occur in a similar temporal range in the video sequence. Kukleva *et. al.* [61] leverage this fact and use a pretext task of timestamp prediction to learn a temporal embedding. These temporal features are later used to find the potential temporal action clusters and their orders for subsequent action segmentation.

Vidalmata *et. al.* [62] later pointed out that a stand-alone temporal embedding lacks sufficient visual cues and proposed a two-stage pipeline to capture both visual and temporal representations of each frame. The first stage trains visual and temporal embedding models separately; the second stage trains both jointly. The visual embedding is learned with a frame prediction task to predict the feature at a future time $t + s$ based on feature input at current time t , while the temporal embedding model follows [61]. The second stage unites two models by imposing a frame reconstruction loss on the temporal model to predict frame representations that can give the best timestamp prediction.

Also based on the temporal embedding [61], Li *et. al.* [49] exploit the extra temporal relations on the action level by training a binary classifier on whether the input sequence of actions has been shuffled. Concretely, negative sequences are randomly sampled and shuffled while positive sequences remain in their original ordering. The final feature embedding is used for subsequent learning.

6 TEMPORAL AND SEQUENTIAL MODELING

Segmenting actions from the frame-wise features outlined in Section 5 typically requires some additional handling of dynamics or change over time. One approach captures the model directly into the network architecture, *i.e.* as part of a temporal convolutional network (TCN), a recurrent neural network (RNN), or a transformer. Others explicitly apply external models such as HMMs or Generalized Mallows Models. In accordance with the hierarchical structure of these videos, the reasoning of the temporal dynamics can be categorized into frame level and segment level. We denote the frame-level model as temporal modeling and the segment-level model as sequential modeling.

6.1 Temporal Modeling

Temporal modeling on a frame-wise basis expands the temporal receptive field of the network and aggregates

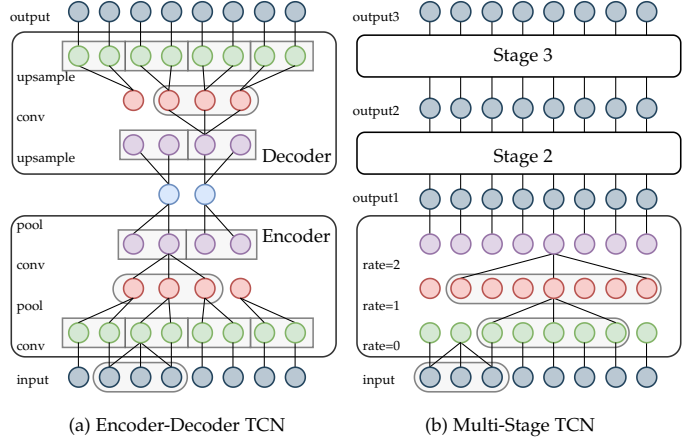


Fig. 5: Two exemplary types of Temporal Convolutional Networks (TCN) for temporal action segmentation. a) Encoder-decoder TCNs progressively enlarge the temporal receptive field via pooling. b) Multi-stage TCNs maintain a fixed temporal resolution with progressively larger dilated convolutions.

the dynamics in the feature representations. This level of modeling is necessary as commonly adopted pre-computed frame representations for TAS were originally designed for action recognition on few-second-long video clips. Several works [74], [75], [76], [77] have shown that these features exhibit bias towards static cues, such as objects, scenes, and people. Efforts dedicated to this problem include Recurrent Neural Networks, Temporal Convolutional Networks, and Transformers.

6.1.1 Recurrent Neural Networks (RNNs)

RNNs attempt to capture the temporal relations by encoding the complete sequence with the same set of shared parameters over time. Among them, Gated Recurrent Units (GRUs) [78] have been adopted in [79], [80]. Specifically, the GRU takes in frame inputs recurrently following their temporal order and predicts action labels. A similar GRU structure is used in [80] as the backbone, while they enable the bidirectional flow of the frames.

The memory of a frame-wise RNN stand-alone does not span long enough to capture the sequential relationship between actions. Above discussed methods [79], [80] are therefore usually combined with sequential modeling techniques which we introduce in Section 6.2. Another weakness of RNN is its limited ability in processing sequential inputs in parallel due to the recurrent dependencies between frames.

6.1.2 Temporal Convolutional Networks (TCNs)

Temporal Convolution Networks (TCNs) [46] use 1D convolutional kernels in time. Two standard paradigms of TCNs, shown in Fig. 5, are encoder-decoders and multi-stage TCNs. Encoder-decoder TCNs [46], [81], [82], [83] shrink and then expand the temporal resolution with layer-wise pooling and upsampling in a U-Net fashion [84]. Alternatively, the multi-stage architecture (MS-TCN) keeps a constant temporal resolutions and expands the receptive field with progressively larger dilated convolutions [14], [85]. Comparatively, the encoder-decoder architecture greatly reduces the computation time of long input sequences with

temporal pooling. However, pooling may harm the prediction accuracy at action boundaries. On the contrary, the MS-TCN architecture preserves the full temporal resolution, especially the boundary information, at the cost of higher computation.

6.1.3 Transformer

Transformers have seen a quick adoption for video tasks, including for TAS. The core technique of a transformer is its attention mechanism; and Sener *et. al.* [86] proposed one of the first attention-based architectures called Temporal Aggregates. The Temporal Aggregates model used the non-local operation [87] to estimate the mutual attention between frames in multiple time spans and fused these together with further attention operations.

ASFormer [88] was one of the first true transformer architectures for TAS. It adopted an encoder-decoder like the ED-TCN [46] and replaced the convolutional operations with a transformer block. In the encoder, the transformer only attends to frames within the inputs, which is often referred as self-attention (SA), while the blocks in the decoder adopt cross-attention (CA) between features and the encoder outputs (see Fig. 6). Building on top of ASFormer, Behrmann *et. al.* [89] adjusts the decoder to output only the action sequence instead of frame-wise action labels, *i.e.*, mapping frame inputs to action sequence outputs.

Transformers are being embraced gradually for TAS, but their use is still limited. First, the transformers lack inductive biases, requiring a large corpus of videos for effective training. Yet existing datasets for TAS are relatively small, making it difficult for large transformers to develop effective representations. Another issue identified by [90] is that the self-attention mechanism might not acquire meaningful weights from a large span of inputs.

In summary, the temporal relationships for action recognition is modelled implicitly through the network architecture. Given the temporal convolution and attention operations discussed above, it is necessary for them to have access to the fine-grained frame-level annotation. Moreover, accurate action boundaries are of more importance to the model for learning ambiguities during action transitions.

6.2 Sequential Modeling

The actions in procedural videos typically follow some sequential order to serve a purpose or achieve a specific goal. Such sequential information is more easily captured on a segment level and various models such as Hidden Markov Models and Mallows Models have been investigated in the existing works [12], [52], [61].

6.2.1 Hidden Markov Model

Hidden Markov Models (HMMs) are classic probabilistic models for working with sequential data input and they have also been applied to model the progression or sequential relations of action segments in video sequences. Recall that for a given video x , TAS is to find the optimal segments $(\hat{c}, \hat{\ell})$, where $\hat{c} = [\hat{c}_1, \dots, \hat{c}_n, \dots, \hat{c}_{\hat{N}}]$ denotes the predicted ordering of action labels of length \hat{N} , $\hat{c}_n \in \mathcal{C}$, and

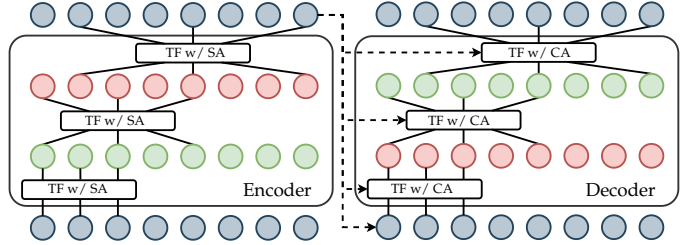


Fig. 6: Transformer architecture proposed for temporal action segmentation. The transformer blocks (TF) takes as input frames with increasing temporal dilation ratios d . The transformers in encoder uses self-attention (SA) across the frames. The decoder takes as input encoder outputs and uses cross-attention (CA) with them at each layer.

$\hat{\ell} = [\hat{\ell}_1, \dots, \hat{\ell}_{\hat{N}}]$ are their corresponding temporal extents. The HMM to estimate the MAP $(\hat{c}, \hat{\ell})$ can be written as:

$$\begin{aligned} (\hat{N}, \hat{c}, \hat{\ell}) &= \arg \max_{N, c, \ell} p(c, \ell | x) \\ &= \arg \max_{N, c, \ell} p(c) \cdot p(\ell | c) \cdot p(x | c) \\ &= \arg \max_{N, c, \ell} \underbrace{\left[\prod_{n=1}^{N-1} p(c_{n+1} | c_n) \right]}_{\text{context model}} \cdot \underbrace{\left[\prod_{n=1}^N p(\ell_n | c_n) \right]}_{\text{length model}} \cdot \underbrace{\left[\prod_{t=1}^T p(x_t | c_n) \right]}_{\text{visual model}}. \end{aligned} \quad (15)$$

The last term $p(x | c)$ in the second line is simplified from $p(x | c, \ell)$ since it is a frame-wise likelihood and does not depend on the action length ℓ .

The HMM formulation induces a three component model. The first, $p(c)$, is a *context model*, providing probabilities for the sequence of actions in the video. As discussed in Section 5.2.3, CTE [61] assumes that similar actions happen in close temporal vicinity so that the average timestamp $t(k)$ for feature clusters in the temporal embedding space is a good indication of the action order in the sequence:

$$t(k) = \frac{1}{|\mathbf{F}(k)|} \sum_{f \in \mathbf{F}(k)} t(f) \quad (16)$$

where $\mathbf{F}(k)$ is the set of features in cluster k and $t(\cdot)$ indicates the normalized temporal location. The clusters are then ordered as $\pi = [k_1, \dots, k_K]$ with respect to their temporal location, such that $0 \leq t(k_1) \leq \dots \leq t(k_K) \leq 1$. With this ordering, the transition probability is defined:

$$p(c_{n+1} | c_n) = \begin{cases} 1, & c_{n+1} = c_n \text{ or } k_{c_{n+1}} - k_{c_n} = 1, \\ 0, & \text{otherwise.} \end{cases} \quad (17)$$

Eq. (17) imposes a hard transition; new frames must either keep the same action label as the previous frame or transition to the next action label observed in the ordering π . Comparatively, Li *et. al.* [49] define a relaxed version, taking into consideration the action length λ_c :

$$p(c_{n+1} | c_n) \propto \begin{cases} \frac{\lambda_{c_n} + \lambda_{c_{n+1}}}{\sum_{j=c_n}^{c_{n+1}} \lambda_{c_j}}, & k_{c_{n+1}} > k_{c_n}, \\ 0, & \text{otherwise.} \end{cases} \quad (18)$$

This formulation allows for the skipping of actions in the ordering π and penalizes multiple action skips with a large denominator (sum of skipped action lengths) in Eq. (18).

The second component $p(l|c)$, the *length model*, determines the temporal length for each action class. Common practice [12], [13], [49], [56] is to model the length of each action with a Poisson distribution:

$$p(l|c) = \frac{\lambda_c^l}{l!} e^{-\lambda_c}. \quad (19)$$

The lengths λ_c for actions are estimated over all video sequences by the following:

$$\hat{\lambda} = \arg \min_{\lambda} \sum_{x \in X} \left(\sum_{c \in \mathcal{A}_x} \lambda_c - T_x \right)^2, \quad \text{s.t. } \lambda_c > \lambda_{\min} \quad (20)$$

where \mathcal{A}_x is the set of occurring actions in video x with T_x frames and λ_{\min} denotes a pre-set minimum length over all actions. This ensures the minimum difference between estimated lengths by summing composing λ_c and actual length T_x over the video set and can be solved with constrained optimization by linear approximation (COBYLA) [91]. Such explicit modeling of lengths is necessary to avoid producing unreasonably long action segments.

The third component, the *visual model*, provides the probability of a feature sequence \mathbf{x} being generated by the given action labels \mathbf{c} . There are multiple ways to model the frame likelihood. Following Bayes' theorem, [12] proposes estimating $p(x_t|c_n)$ by considering:

$$p(x_t|c_n) \propto \frac{p(c_n|x_t)}{p(c_n)}, \quad (21)$$

where prior $p(c_n)$ can be estimated either by the fraction of frames present with label c_n [13] or as a uniform distribution for simplicity [49], while the posterior $p(c_n|x_t)$ are approximated by the output of an action classification network supervised by the action annotations.

Generative models like GMMs can also be used to model the frame likelihood. In the GMM, the likelihood for a video frame x_t to be given an action class c_n is written as:

$$p(x_t|c_n) = \mathcal{N}(x_t; \mu_n, \Sigma_n) \quad (22)$$

where μ_n and Σ_n are the action class mean and covariance. In practice, GMMs are preferred for cases where no action annotations are available [61], [62].

Viterbi. The MAP for the HMM described in Eq. (15) can be solved efficiently with the Viterbi algorithm [92]. Viterbi relies on dynamic programming to find the most likely sequence of states following the temporal direction. Consider the case where a uniform length model applied in Eq. (15) yields the following:

$$(\hat{N}, \hat{\mathbf{c}}) = \arg \max_{N, \mathbf{c}} \prod_{n=1}^{N-1} p(c_{n+1}|c_n) \cdot \prod_{t=1}^T p(x_t|c_n). \quad (23)$$

which can be further rewritten by denoting the labeling sequence of T frames π :

$$\hat{\pi} = \arg \max_{\pi} \prod_{t=1}^T p(x_t|\pi_t) \cdot p(\pi_t|\pi_{t-1}) \quad (24)$$

Given the recurrence relations, we can define the probability value $Q_{t, \hat{\pi}_t}$ of the most probable state sequence, also called the Viterbi path, as:

$$Q_{1, \pi_1} = p(x_1|\pi_1) \cdot p(\pi_1) \quad \text{and} \quad (25)$$

$$Q_{t, \hat{\pi}_t} = \max_{\pi_t} (p(x_t|\pi_t) \cdot p(\pi_t|\pi_{t-1}) \cdot Q_{t-1, \hat{\pi}_{t-1}}). \quad (26)$$

Then Viterbi path $\hat{\pi}$ can be retrieved by traversing the saved best $\hat{\pi}_t$ from each timestamp in Eq. (26). The overall complexity of this implementation is $\mathcal{O}(T \times |N|^2)$.

Re-estimation. [49], [61] have stated that the aforementioned HMM model can be updated iteratively. As a first step, one initializes the above three HMM components with naive observations. Second, the Viterbi decoding is applied to infer the MAP label sequence. The decoded labels can again be applied to refine the feature inputs to the HMM components. These steps can be repeated until convergence.

Inference. To reduce the computational complexity of Viterbi, [93] proposed FIFA. Instead of dynamic programming, [93] defines a differentiable energy function to approximate the probabilities of possible segment alignments. Their inference process reformulates the maximization of the sequence posterior by minimizing the proposed energy function. Given the transcript $c_{1:N}$, the aim is to find the lengths $\ell_{1:N}$ correspondingly, *i.e.*,

$$\begin{aligned} \hat{\ell}_{1:N} &= \arg \max_{\ell_{1:N}} p(\ell_{1:N}|x_{1:T}, c_{1:N}) \\ &= \arg \min_{\ell_{1:N}} -\log p(\ell_{1:N}|x_{1:T}, c_{1:N}) \\ &= \arg \min_{\ell_{1:N}} E(\hat{\ell}_{1:N}). \end{aligned} \quad (27)$$

The objective energy function $E(\ell_{1:N})$ can be further decomposed as

$$\begin{aligned} E(\ell_{1:N}) &= -\log \left(\prod_{t=1}^T p(\alpha(t)|x_t) \cdot \prod_{n=1}^N p(\ell_n|c_n) \right) \\ &= \underbrace{\sum_{t=1}^T -\log p(\alpha(t)|x_t)}_{E_\alpha} + \underbrace{\sum_{n=1}^N -\log p(\ell_n|c_n)}_{E_\ell}. \end{aligned} \quad (28)$$

where $p(\alpha(t)) = p(y_t|t; c_{1:N}, \ell_{1:N})$ is the mapping of time t to action label given the segment-wise labeling, and $c_{1:N}$ is sampled from the training set as mentioned in Section 4.3.

Two further approximations are used for the two terms in Eq. (28). First is a differentiable mask $M \in \mathbb{R}^{N \times T}$ with a parametric plateau function f [94]:

$$\begin{aligned} M[n, t] &= f(t|\lambda_n^c, \lambda_n^w, \lambda^s) \\ &= \frac{1}{(e^{\lambda^s(t-\lambda_n^c-\lambda_n^w)} + 1)(e^{\lambda^s(-t+\lambda_n^c-\lambda_n^w)} + 1)} \end{aligned} \quad (29)$$

where λ^c, λ^w are the center and lengths of a plateau computed from $\ell_{1:N}$ and λ^s is a fixed sharpness parameter. Hence, the first term E_α is approximated as:

$$E_\alpha^* = \sum_{t=1}^T \sum_{n=1}^N M[n, t] \cdot P[n, t] \quad (30)$$

where $P[n, t] = -\log p(c_n|x_t)$ is the negative log probabilities. Secondly, for E_ℓ , c_n is replaced with the expected length value $\lambda_{c_n}^l$ based on a Laplace distribution assumption:

$$E_\ell^* = \frac{1}{Z} \sum_{n=1}^N |\ell_n - \lambda_{c_n}^l| \quad (31)$$

where Z is the constant normalization factor. The original energy function is finally expressed as a weighted aggregation of two approximation terms:

$$E^*(\ell_{1:N}) = E_o^*(\ell_{1:N}) + \beta E_\ell^*(\ell_{1:N}) \quad (32)$$

where β is a coefficient. FIFA can boost the inference speed up to $5\times$ and at the same time maintain a comparable performance score.

6.2.2 Generalized Mallows Model

A generalized Mallows Model (gMM) models distributions over orderings or permutations. Given a set of videos belonging to the same activity, Sener *et. al.* [52] propose using a gMM to model the sequential structures of actions for action segmentation. Their assumption is that a canonical sequence ordering σ is shared in these videos and they consider possible action ordering π as a permutation of σ . Such modeling offers flexibility for missing steps and deviations. A gMM represents permutations as a vector of inversion counts $v = [v_1, \dots, v_{K-1}]$, where K is the number of elements, *i.e.* actions, in the ordering and v_k denotes the total number of elements from $(k+1, \dots, K)$ that rank before k in the ordering π . With the distance between two orderings defined as $d(\pi, \sigma) = \sum_k \rho_k v_k$, the probability of observing v is as follows:

$$P_{GMM}(v|\rho) = \frac{e^{-\sum_k \rho_k v_k}}{\psi_k(\rho)} = \prod_{k=1}^{K-1} \frac{e^{-\rho_k v_k}}{\psi_k(\rho_k)}, \quad (33)$$

where $\rho = [\rho_1, \dots, \rho_{K-1}]$ is a set of dispersion parameters and $\psi_k(\rho_k)$ is the normalization function. The prior for each ρ_k is the conjugate:

$$P(\rho_k|v_{k,0}, v_0) \propto e^{-\rho_k v_{k,0} - \log(\psi_k(\rho_k))v_0}, \quad (34)$$

A common prior ρ_0 is used for each k , such that

$$v_{k,0} = \frac{1}{e^{\rho_0}} - \frac{K-k+1}{e^{(K-k+1)\rho_0} - 1}. \quad (35)$$

Given an action ordering π , generating frame-wise label assignment z further requires an action appearance model a . a is the bag of action labels providing the occurrence for each action and is modeled as a multinomial parameterized by θ and a Dirichlet prior with parameter θ_0 .

Recall that the assumption in the work of [52] is that the canonical ordering is given, thus their objective is to infer the following posterior over the entire video corpus,

$$P(z, \rho|F, \theta_0, \rho_0, v_0) \propto P(F|z)P(a|\theta)P(\theta|\theta_0)P(\rho|\rho_0, v_0) \quad (36)$$

where F is the frame features. The feature likelihood term $P(F|z)$ is evaluated with GMM (Eq. (22)) and the remaining terms are approximated via MCMC sampling. Specifically, they use slice sampling for ρ and collapsed Gibbs sampling for z . Similar to HMM, the above model can also be trained in two stages, where discriminative feature clustering (as described in Section 5.2.1) and sequential modeling are performed in an alternating fashion.

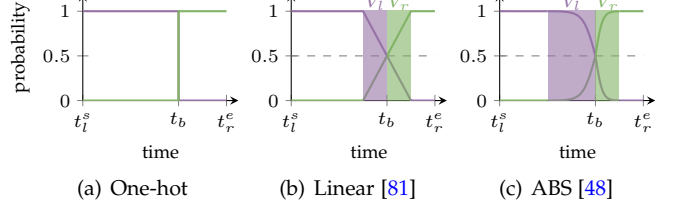


Fig. 7: Action probability assignment approaches around the action boundary as a function of time. Let t_b denote the estimated boundary between the left action in $[t_l^s, t_b)$ and the right action $[t_b, t_r^e)$. The colour-shaded segments denote the boundary vicinities V_l and V_r . (a) One-hot labels adopt a step function with hard action labels assignments. (b) Linear [81] linearly mixes the action probabilities. (c) ABS [48] uses a sigmoid function with a decay proportional to the action duration.

6.2.3 Dynamic Time Warping

Other than Viterbi, dynamic time warping (DTW) has also been used in the literature to implement sequential modeling. SemiTAS [48] first sub-samples in time an ordered action sequence from the frame-wise network prediction, and then computes a cost matrix between the sequence and frame predictions to enforce the sampled sequential order of actions. The proposed continuity loss is to compute the loss along the optimal assignment path found via DTW.

6.3 Over-Segmentation

Local continuity is an inherent attribute of procedural actions, meaning an action should be locally continuous and only change at its actual boundary. This has motivated researchers to refine the results of existing segmentation algorithms at the boundaries to increase their performance.

Boundary Refinement. Wang *et. al.* [95] raise concerns over the boundary ambiguity and over-segmentation issues in existing works and propose a module for multi-stage segmentation algorithms [14]. Their module enables the later stages to smooth noisy boundary predictions with confident ones with a novel Local Barrier Pooling operation. Separately, [96] proposes to supplement the segmentation branch with a boundary regression branch, and use boundary detection on the segmentation outputs for post-processing.

Gaussian Smoothing. Smoothing with a Gaussian kernel [51], [54], [96] promotes the continuity of actions in a narrow local temporal window and is highly effective in enhancing segmentation performances, especially on the segmental metrics. While [51], [96] directly apply smoothing on the frame-wise action probabilities, Du *et. al.* [54] apply it along the temporal dimension of sequential similarity scores between consecutive frames to mitigate the noisy frames and obtain more robust boundaries.

Boundary Smoothing. From a different perspective, some research suggests that coarser transitional action boundaries may improve the TAS performance compared to the conventional rigid ones [48], [81]. A comparison of existing boundary smoothing techniques proposed for TAS is illustrated in Fig. 7. Correspondingly, [81] mixes the action probabilities with a fixed slope linear decay (Fig. 7(b)), whereas [48] elastically expands the smoothing range to be

proportionate to the estimated action duration and employs a sigmoid shape for mixing (Fig. 7(c)).

7 FULLY-SUPERVISED APPROACHES

Supervised TAS approach requires frame-wise action labels during training. Following the trend of other developments in action recognition, supervised TAS research has moved towards adopting deep learning-based solutions. Early approaches before deep-learning-based solutions to TAS classified actions in a temporal sliding window [106], [107], [108]. Among these, Cheng *et. al.* [108] reason on the dependencies between the actions with a Bayesian non-parametric language model. In contrast, [109], [110] model the actions as a change in the state of objects and approached the segmentation problem as finding change points.

Another line of methods before deep learning approaches predicts the most probable sequence of actions using stochastic context-free grammar to represent the temporal structure of actions [111], [112] and combining a set of hidden Markov models with a context-free grammar [28], [100]. [113] combines a visual model that maps visual cues to action probability with a language model applied to the action sequence and captures the segment durations with a length model. Finding the final segmentation output that optimizes the likelihood of all three components is performed via dynamic programming.

This section discusses deep models utilized for TAS. Taxonomically, we identify four main categories in the following text. The performance of these approaches is compared in Tab. 7 on the Breakfast and GTEA. Overall, we find that the majority of the approaches are TCN-based. Although several types of features were used in the early approaches, I3D features are mostly employed to achieve the current state of the art.

7.1 Representation Learning

The early attempts combine features derived from deep learning with temporal models. Lea *et. al.* [55] utilize a CNN to capture spatiotemporal feature relations (ST-CNN) and a semi-Markov model to segment videos. To compute visual representation, Bi-LSTM [97] divides videos into snippets and passes them through a multi-stream network composed of appearance and motion streams. Then, these features are fed into a bi-directional LSTM to predict action labels.

The focus of follow-up works is on acquiring better representations for fine-grained actions. Instead of optical flow, [98] models fine-grained motion with locally consistent deformable convolutions (LCDC). Coupled GAN [99] models the evolution of actions with two generative adversarial networks, one for RGB images and one for auxiliary information (depth or optical flow).

TempAgg [86] is a recent framework for multi-granular temporal aggregation that relates recent observations to long-range ones with attention. This network can be used for TAS by naively classifying long-range information-aggregated snippets. Although performance is reported only based on snippet scores, adding a sequence model is expected to result in further improvements.

7.2 Temporal Convolutional Networks (TCNs)

Temporal patterns are captured by TCNs via a hierarchy of convolutions. Lea *et. al.* [46] were the pioneers in implementing TCNs for TAS. They present an encoder-decoder architecture (ED-TCN) with 1D temporal convolutional and deconvolutional kernels that capture long-range temporal patterns. In addition to capturing action durations, pairwise transitions, and long-term dependencies, TCN-based solutions are fast.

TricorNet [11] substitutes a bi-directional LSTM for the decoder in ED-TCN and offers a hybrid temporal convolutional and recurrent network. Due to the recurrences, this network incurs large computation costs. Moreover, TDRN [82] builds upon ED-TCN by substituting the temporal convolutions with deformable temporal convolutions and by adding a residual stream to the encoder-decoder model. The residual stream processes videos with the full temporal resolution, while the other stream collects the temporal context at various scales.

Although the above TCN-based approaches work on the entire video, referred to as *full resolution*, in reality, these methods temporally downsample the videos to a few frames per second. This type of pre-processing may cause the loss of fine-grained details. In contrast, Farha and Gall [14] propose MS-TCN, a multi-stage hierarchical temporal convolutional network that works on exact full-resolution video. Each stage of MS-TCN comprises multiple temporal convolutional layers with 1D dilated convolutions and outputs an initial prediction that is iteratively refined by subsequent stages. This work considerably enhances the segmentation performance compared to earlier works [46], [82] by a large margin and lowers over-segmentation mistakes.

MS-TCN++ [85] introduces a dual dilated layer and shares parameters in refining stages to improve upon MS-TCN. RPGaussian [101] presents a bilinear pooling module that is integrated into TCNs to serve as an efficient feature fusion operation, *e.g.*, by replacing the last 1×1 convolution layer in the first stage of MS-TCN. GatedR [102] employs a gated forward refinement network to correct errors from the previous stages in an adaptive manner. It also incorporates a multi-stage sequence-level refinement loss to correct the errors in the previous predictions.

An analysis of fragmentation concerns in TCNs by Singhania *et. al.* [83] leads to the development of the C2F-TCN encoder-decoder model with a coarse-to-fine ensemble of decoding layers. Its decoder output ensemble is less fragmented and more precise. This work also introduces a multi-resolution feature-level augmentation strategy and an action loss that penalizes misclassifications at the video level, hence improving segmentation performance.

7.3 Improving Existing Architectures or Outputs

Several efforts concentrate on enhancing existing TAS algorithms by incorporating new modules into existing backbones or by post-processing the outputs. Chen *et. al.* [104] argue that spatiotemporal variations of human actions referred to as *different domains*, lead to poor performance in supervised TAS, as training a model in one domain and testing it in another will fail due to the variation gap. They propose to employ two self-supervised auxiliary tasks to

TABLE 7: Performance of supervised TAS methods on the Breakfast and GTEA. **Rep.** corresponds to approaches targeting learning better feature representations. **TCN** lists methods built on Temporal Convolutional Networks. **Impro.** group aims to improve the performance of existing algorithms. Lastly, **TF** uses transformer as the backbone. **FT** means fine-tuning.

Method	Year	Input/Feature	GTEA			Breakfast		
			F1@{10, 25, 50}	Edit	MoF	F1@{10, 25, 50}	Edit	MoF
Rep.	[97] Bi-LSTM	2016	RGB + flow	66.5	59.0	43.6	-	55.5
	[55] ST-CNN	2016	RGB + motion*	58.7	54.4	41.9	-	60.6
	[98] LCDC	2019	RGB	52.4	-	45.4	55.3	-
	[99] Coupled GAN	2019	RGB + flow	80.1	77.9	69.1	72.8	78.5
	[86] TempAgg	2020	I3D	-	-	-	-	-
TCN	[46] ED-TCN	2017	LCDC [98]	75.4	-	-	72.8	65.3
	[46] ED-TCN	2017	IDT + FV [100]	-	-	-	-	-
	[46] ED-TCN	2017	spatial-CNN [55]	72.2	69.3	56.0	-	64.0
	[11] TricorNet	2017	spatial-CNN [55]	76.0	71.1	59.2	-	64.8
	[82] TDRN	2018	spatial-CNN [55]	79.2	74.4	62.7	74.1	70.1
	[14] MS-TCN	2019	IDT	-	-	-	-	-
	[14] MS-TCN	2019	I3D (FT)	87.5	85.4	74.6	81.4	79.2
	[14] MS-TCN	2019	I3D	85.8	83.4	69.8	79.0	76.3
	[85] MS-TCN++	2020	I3D	87.8	86.2	74.4	82.6	78.9
	[101] RPGaussian	2019	I3D	88.5	86.8	74.6	84.0	78.5
	[102] GatedR	2020	I3D	89.1	87.5	72.8	83.5	76.7
	[83] C2F-TCN	2021	I3D	90.3	88.8	77.7	86.4	80.8
TF	[88] ASFormer	2021	I3D	90.1	88.8	79.2	84.6	79.7
TF	[89] UVAST	2022	I3D	77.1	69.7	54.2	90.5	62.2

* Motion images are computed by taking the difference between frames across a 2 second window.

** The improvements are computed based on the authors' implementation of MS-TCN.

† Test set without labels is used for training.

reduce discrepancies between source and target domains' feature space. One task predicts which domain a single frame's feature vector originates, while the other predicts domain labels for a shuffled *sequence* of source and target segments. Combining their self-supervised model, SSTDA, with MS-TCN significantly improves the performance without the use of extra labeled data. Such superior performance could potentially benefit from having access to the test data as the unlabeled inputs.

GTRM [80] refines segmentation outputs generated by conventional TAS methods using a graph convolutional network (GCNs). The refinement depends on the quality and degree of fragmentation of initial segmentation. In segmentation models, temporal receptive fields are crucial, with large fields facilitating long-term relations and small receptive fields capturing local changes. In lieu of manually created receptive fields, Global2Local [105] introduces a search scheme for effective receptive field combinations that can be inserted into any existing segmentation model.

Correction of segmentation findings at action boundaries is a second suggestion for improvement. Wang *et. al.* [95] raise concerns over the boundary ambiguity and over-segmentation issues in previous works and specifically propose a module that can be used with MS-TCN. Their module, BCN, enables the later stages to focus on ambiguous frames. A newly designed pooling operator smooths noisy boundary predictions with confident ones. Similarly, ASRF [96] also does boundary refinement, but it is model-independent and may be applied to any TAS output.

7.4 Transformers

Transformers have recently been utilized for TAS. ASFormer [88] is a transformer-based segmentation model with an encoder and multiple decoders to perform iterative refining. A self-attention block with instance normalization is used per dilated temporal convolutional layer of MS-TCN. The initial stage is the encoder, which takes the video sequences and outputs predictions, while the decoders receive as input the predictions from preceding layers. On GTEA, ASFormer performs on par with MS-TCN, while on Breakfast, it outperforms MS-TCN. Another recent work, UVAST [89], uses a similar encoder but a different decoder than ASFormer. UVAST's decoder predicts the action segments in an auto-regressive way, as opposed to ASFormer and MS-TCN, which do frame-level predictions. On F1-score and Edit Score, UVAST surpasses previous methods, suggesting reduced over-segmentation.

8 WEAKLY-SUPERVISED APPROACHES

The objective of weakly supervised techniques is to avoid intensive frame-level supervision. We classify these techniques into five categories. One group receives supervision in the form of an ordered list of actions known as *transcripts*. The second one uses an unordered list of actions called *action sets*. The third group labels each video with action timestamps. The fourth is even weaker supervision as it only accepts complex activity labels. The fifth and final category consists of segmentation methods that leverage

complementary *textual data* such as narrations to provide temporal constraints. We compare the performance of all approaches on Breakfast and 50Salads in Tab. 8.

8.1 Transcripts: Ordered List of Actions

Kuehne *et. al.* [114] were the first to use the term *transcripts* to refer to an ordered list of the actions occurring in a video. Even earlier work already features transcripts [115], however, it focuses on aligning frames with the transcripts and assumes that the test transcripts sequences are also provided.

Transcript-based supervision gives simply the actions within a video and their chronological order. This type of supervision significantly reduces the cost of annotating videos because it does not require any frame-by-frame labels, and it could accelerate the annotation of Breakfast by an order of magnitude. We categorize these methods into iterative two-stage and single-state solutions.

8.1.1 Iterative Two-Stage Solutions

The two-stage solutions begin with an initial estimate of frame-wise labels, which is subsequently improved iteratively using a segmentation model. These methods are based on an incremental refinement of previous predictions. HTK [114] extends an approach from supervised [100] to weakly-supervised setting. A set of HMMs represents the actions in this framework, whereas a GMM models the observations. The algorithm uniformly initializes and iteratively refines the video segments depending on the transcripts. On the basis of this concept, Richard *et. al.* [79] replaces GMMs with recurrent neural networks. Additionally, they subdivide the actions into fragments to capture their finer properties.

ISBA [81] expands the TCN from [46] by adding encoder and decoder layer lateral connections. They employ a soft labeling method at the segment boundaries and refine the segmentation iteratively. TASL [116] offers to model the action subspaces with an ensemble of auto-encoders and a similar two-stage strategy of iterating between aligning videos with regard to transcripts and learning subspace learning with the alignment. In particular, a constrained Viterbi decoding algorithm [12], [56] is utilized to efficiently tackle the alignment problem.

8.1.2 Single-Stage Solutions

The two-step approaches are initialization-sensitive and may not converge when the models are incrementally trained. Segmentation can be learned directly through single-stage techniques. ECTC [117] is an extended variant of connectionist temporal classification [118] for aligning the transcripts with video frames under consistency restrictions. It ensures frame-wise similarities so that the action alignments are consistent. This lowers the space of viable pathways and prevents degenerate segmentation, which could result from a large number of frames in long videos.

NN-Viterbi [12] employs Viterbi decoding as part of the loss function to train a segmentation network. The Viterbi algorithm generates pseudo-ground truths for the network's output probabilities, which are subsequently used to calculate the loss. This method presents a substantial advance

over the previous methods. Yet, training is expensive due to Viterbi decoding. Chang *et. al.* [119] propose D³TW, a framework with a differentiable alignment loss to model positive and negative transcripts discriminatively. Similar discriminative training is proposed by Li *et. al.* [120], whose framework, CDFL, is constructed on NN-Viterbi with ordering restrictions. CDFL, unlike D³TW, generates valid and invalid segmentation candidates using a segmentation graph, where invalid candidates violate the transcripts. It formulates a new loss based on the energy differences between valid and invalid candidates using a recursive estimation of each candidate's segmentation energy. CDFL performs far better than is predecessors, although its training is more costly.

Souri *et. al.* [121] call attention to the lengthy training time of the state-of-the-art and propose a sequence-to-sequence network that performs comparably to previous research but is significantly faster during training and inference. Their framework, MuCon, consists of two branches, one of which produces frame-wise predictions while the other predicts transcripts with durations. Using the predictions from the two branches, a mutual consistency loss is computed to ensure comparable predictions. A recent work, DP-DTW [122], trains class-specific discriminative action prototypes for weakly-supervised segmentation and suggests that videos could be represented by concatenating prototypes based on transcripts. The model seeks to increase the inter-class distinction between prototypes by means of discriminative losses.

8.2 Action Set

Action set assumes that a collection of action labels is presented for training without knowledge of their temporal location, order, or frequency. This type of labeling may appear as meta-tags on video-sharing platforms, for example.

Richard *et. al.* [13] are the first to propose a weak segmentation model based on action sets. Similar to [113], their structure consists of an action, length, and sequence component and employs Viterbi to determine the most probable segmentation. They produce several transcripts utilizing context-free grammar to limit the search space and transform the problem into a weakly-supervised setting with multiple transcripts. However, this work cannot generate all possible sequences of an action set, which might compromise the quality of segmentation.

SCT [123] learns a segmentation network that uses annotations directly for learning. They begin by segmenting videos into regions, then estimate action probabilities and temporal lengths with one branch. A second branch is utilized to provide frame-wise predictions. They measure the consistency of the frame-wise predictions with regard to region predictions, which considerably increases the accuracy of the model. In addition, they define several losses and regularizers to encourage temporally consistent predictions between adjacent regions or regularize region lengths.

SCV [56] uses a set-constrained Viterbi algorithm to generate accurate pseudo ground truths and an n -pair loss to minimize the distance between training video pairs that share action classes in respective action sets. It employs a greedy post-processing step to ensure that all actions are included in the frame-wise pseudo-ground truth by replacing

TABLE 8: Performance of weakly supervised methods on Breakfast and 50Salads. **Tr.** indicates transcripts supervision. **T** groups iterative two-stage solutions, while **S** single-stage solutions. Action set is denoted by **Set**. **TS** provides timestamp annotation for frames. **CA** stands for complex activity.

Method	Year	Feature	Breakfast			50Salads
			MoF	IoU	IoD	
Tr. + T	[114] HTK	2017	IDT + FV	25.9	-	-
	[79] HMM/RNN	2017	IDT + FV	33.3	-	45.5
	[81] ISBA	2018	IDT + FV	38.4	24.2	40.6
	[116] TASL	2021	IDT + FV	49.9	36.6	34.3
Tr. + S	[117] ECTC	2016	IDT + FV	27.7	-	-
	[121] NN-Viterbi	2018	IDT + FV	42.9	32.2	29.1
	[119] D ³ TW	2019	IDT + FV	45.7	-	-
	[120] CDFL	2019	IDT + FV	50.2	33.7	45.4
	[121] MuCon	2019	IDT + FV	48.5	-	-
	[122] DP-DTW	2021	IDT + FV	50.8	35.6	45.1
Set	[13] ActionSet	2018	IDT + FV	23.3	-	-
	[123] SCT	2020	IDT + FV	26.6	-	-
	[123] SCT	2020	I3D	30.4	-	-
	[56] SCV	2020	IDT + FV	30.2	-	-
	[124] ACV	2021	IDT + FV	33.4	-	-
TS	[126] Timestamps	2021	I3D	64.1	-	75.6
	[50] EM-TSS	2022	I3D	63.7	-	75.9
CA	[51] CAD	2022	IDT+FV	49.5	-	-
	[51] CAD	2022	I3D	53.1	-	-

low-score frames with action labels included in the action set but absent from the initial segmentation. ACV [124] improves this work by eliminating the necessity for post-processing by use of differentiable approximation that allows end-to-end training. It builds an anchor-constrained graph and estimates anchor segments to confine the candidate set of valid sequences.

Recent observations by Lu *et. al.* [125] indicate that it is typical for action pairs to have a fixed temporal order in multiple procedural videos, which could help improve the segmentation performance. In light of this, they incorporate these constraints into learning using a pairwise order consistency loss. The loss penalizes the ordering disagreement between extracted templates and outputs of the segmentation model outputs.

8.3 Single-Frame Supervision

Instead of annotating every frame with an action label, another type of supervision obtains labels from single timestamps for each action, significantly lowering the effort required for annotation. The annotation could correspond to any arbitrary frame for each segment.

Li *et. al.* [126] present a method for generating frame-wise labels by detecting action transitions. They implement a confidence loss that mandates the class probabilities to decrease monotonically as the distance to the timestamp grows. Their method is applicable to any TAS model for training. Compared to using transcripts or action set-based weak supervision, this type of supervision greatly improves the segmentation performance. Its performance is comparable to that of fully supervised, making it an intriguing direction to explore.

Recently, Rahaman *et. al.* [50] proposed incorporating Expectation-Maximization (EM) for timestamp supervision with the notion that the missing frame labels might be deduced from labeled timestamps. The E-step is designed to train the network for the label estimation, whereas the M-step maximizes the timestamp segment likelihood and

calculates the boundary based on this maximization. They illustrate the generalizability of the proposed EM approach to manage the missing actions between annotated timestamps. Their model indicates that labeling the initial frame for each segment impairs performances in comparison to a random or middle frame initialization, demonstrating the ambiguity of labels at the boundaries.

Previously stated approaches utilize a segmentation model to help infer the action boundaries that are in between timestamps, whereas GCN [134] proposed adopting the Graph Neural Network (GNN) to achieve the same goal in an alternative manner. Specifically, the frame features are considered as nodes, and the edges between consecutive frames are weighted by their feature affinity, which is computed as the cosine similarity. The GNN is trained to propagate labels from a few labeled nodes to the rest of the unlabeled nodes.

8.4 Narrations & Subtitles

Frequently, videos are accompanied by publicly available text data in the form of scripts, subtitles, or narrations. It is commonly employed for video and text alignment [42], [135] and step localization [22], [34]. Many works make use of text to weakly supervise TAS. The primary drawback of textual data is the assumption that *all* the videos are accompanied by temporally aligned text. Unfortunately, text data may not always be properly aligned and could be absent.

Sener *et. al.* [136] combine visual and language cues in a hybrid generative model to segment videos. They construct object proposal segments and compute visual vocabularies from a collection of videos of the same activity. Combining these along with computed textual vocabularies over narrative text, they represent each frame with a binary histogram of visual and textual words. Using binary data, they employ the generative beta process mixture model from [21] in order to detect the actions shared by multiple videos. They evaluate the proposed method on a newly collected dataset of 17 activities and 5 test videos per activity.

On a separate track, Fried *et. al.* [137] describe a method for segmentation that uses canonical step ordering and transcribed narrations. Canonical step ordering refers to normal order in which the steps of an activity are carried out. They model the segment duration, location, order, and features using a semi-Markov model. Although they do not use the narrations during testing, they use the canonical ordering during inference because these constraints affect the parameters of their model. This work systematically assesses how much models can improve when by increasing the amount of supervision, for as by switching from canonical ordering to narrated transcripts or full supervision. They exclusively provide results for the CrossTask dataset [22] since it includes narratives and canonical orderings for activities, allowing for their methodical examination.

8.5 Activity Supervision

Proposed as an even weaker supervision signal for the TAS task is the use of solely complex activity labels [51]. This type of supervision does not give information at the action level. Ding and Yao [51] propose a Constituent Action Discovery (CAD) framework that learns frame representations

TABLE 9: Performance of unsupervised methods evaluated on the Breakfast Actions dataset. **Two Stg.** indicates the two stages group, and **SS** the self-supervision type. **Single Stg.** list methods with only a single stage. A correspond to activity level evaluation while **V** the video level. We also present how **Temporal Model** is defined and their flexibility for allowing **Deviations**, **Missing** steps and **Repetitions** in orderings.

	Method	Year	Input/Feature	F1(A)	MoF(A)	MoF(V)	Temporal Model	Deviations	Missing	Repetitions
Two Stg.	[52] Mallows	2018	IDT + FV	-	34.6	-	Mallows model [127]	✓	✓	-
	[128] Prism	2019	IDT + FV	-	33.5	-	hierarchical Bayesian model	-	-	✓
	[61] CTE	2019	IDT + FV	26.4	41.8	-	temporal cluster order	-	✓	-
	[62] JVT	2021	IDT + FV	29.9	48.1	52.2	temporal cluster order	-	✓	-
	[51] CAD*	2021	IDT + FV	-	49.5	-	temporal cluster order	-	✓	-
	[51] CAD*	2021	I3D	-	53.1	-	temporal cluster order	-	✓	-
SS	[49] ASAL	2021	IDT + FV	37.9	52.5	-	HMM	-	✓	-
	[129] CAP	2021	SpeedNet [130]	39.2	51.1	-	temporal cluster order	-	✓	✓
Single Stg.	[60] LSTM+AL	2019	CNN [131]	-	-	42.9	-	-	-	-
	[132] UDE	2021	I3D	31.9	47.4	74.6	temporal cluster order	-	✓	-
	[133] TOT	2021	IDT + FV	31.0	47.5	-	temporal optimal transport	-	✓	-
	[53] TW-FINCH	2021	IDT + FV	-	-	62.7	-	-	-	-
	[54] ABD	2022	IDT + FV	-	-	64.0	-	-	-	-

* CAD is included here as it essentially uses same amount of supervision information as the unsupervised approaches.

based on their similarity to the latent action prototypes. They assume that the complex activity label can be inferred using aggregated action prototype affinities across the whole video sequence. Despite being deemed to be weakly supervised, this method uses the same amount of information as the majority of unsupervised works.

9 UNSUPERVISED APPROACHES

For supervision, unsupervised TAS approaches do not require action labels, temporal boundaries, nor textual data. Yet, because of the application scope of their proposed learning strategies, they would implicitly require activity information [52], [61], [136]. Tab. 9 categories existing unsupervised works and evaluates their performances on the Breakfast. The first set of works [52], [61], [62] feature two iterative steps of alternating between frame clusters estimation and frame representations learning. The second group employs self-supervised learning-based representations [49], [129]. The last group disregards sequence dynamics and solely segments depending on boundary changes, *e.g.*, LSTM+AL [60], TW-FINCH [53] and ABD [54]. Interestingly, these methods outperform previous works on unsupervised temporal segmentation. This is likely owing to the limits of the existing datasets, which are either too small to see the effect of modeling the sequence structure [26] or contain activities that predominantly adhere to a rigid ordering [28].

9.1 Two-Stage Learning

Sener and Yao [52] are the first to offer an unsupervised segmentation approach that operates entirely on unsupervised visual data. They propose an iterative discriminative-generative strategy for TAS. Their method alternates between discriminatively learning the action appearance and generatively modeling their temporal structure using a gMM [127]. Although the Mallows framework permits deviations from ordering, such as missing steps, it cannot model depict repeated actions since the ordering of actions is considered as a permutable sequence of steps. Follow-up studies on unsupervised learning are evaluated based on to their flexibility in deviations, missing steps, and ordering

repetitions. For example, Prism [128] is a hierarchical generative Bayesian model that permits repeated actions. This model, however, implies that all the videos adhere to the same underlying ordering.

CTE [61] and JVT [62] outperform the Mallows [52] framework (see Tab. 9). CTE [61] first learns continuous temporal embeddings of frame-wise features. Afterwards, these features are clustered, and the video ordering is decoded using Viterbi. A form of CTE groups videos into activity clusters during the pre-processing phase, rather than receiving activity labels as input. JVT [62] is a joint visual-temporal learning model predicts future frame features using the similar temporal embedding from CTE and an encoder-decoder network. In turn, these two embedding networks are trained in a joint framework to learn useful representations of visual and temporal attributes. The embedding space is then employed for clustering to generate the action segments.

The preceding approaches presuppose a fixed sequential ordering determined by the average timestamp for each cluster. The use of a predetermined order for all videos allows missing steps but cannot accept deviations nor repetitions. CAP [129] offers a method for computing the video order by representing the multi-occurrence of actions using co-occurrence relations. Recent work by Bansal *et. al.* [138] proposes to infer the temporal orderings of the discovered actions per video based on the assumption that there may be multiple ways to complete a given task. In [138], however, the ordering is still based on the average cluster timestamps.

9.2 Self-Supervised Learning

To extract frame-level feature representation in unsupervised learning, Wang *et. al.* [129] propose using self-supervised learning methods. Similar to exiting unsupervised works [61], [62], they first cluster these features. Their method, CAP, decodes the frames into actions using temporal order of actions co-occurrence relations. This enables improved modeling of the activities, by extension, the repetitions. In addition, they compare several self-supervised designs to demonstrate that such feature-learning techniques can increase performance. ASAL [49] provides an efficient approach for the self-supervised learning of feature embeddings through the temporal shuffling of the predicted action

TABLE 10: Performance of semi-supervised methods evaluated on GTEA, Breakfast Actions and 50Salads with varying ratios of labeled data (D%). Abbreviated names are feature learning (FL) that learns a new set of inputs in a self-supervised manner, test data (TD) is used for feature learning, and feature ensembling (FE) technique to boost the performance. Complex acvity indicates the video-level labels used for training (CA), which is only applicable to the Breakfast dataset.

D%	Method	Year	FL	TD	FE	Backbone	Breakfast				50Salads				GTEA							
							CA	F1@{10, 25, 50}	Edit	Acc	F1@{10, 25, 50}	Edit	Acc	F1@{10, 25, 50}	Edit	Acc						
5%	[48] SemiTAS	2022	-	-	-	MS-TCN [14]	-	44.5	35.3	26.54	45.9	38.1	37.4	32.3	25.5	32.9	52.3	59.8	53.6	39.0	55.7	55.8
	[48] SemiTAS	2022	-	-	-	MS-TCN [14]	✓	56.6	49.3	35.8	59.4	56.6	-	-	-	-	-	-	-	-	-	-
	[47] ICC	2022	✓	✓	✓	ED-TCN [46]	-	-	-	-	-	-	39.3	34.4	21.6	32.7	46.4	-	-	-	-	-
	[47] ICC	2022	-	-	✓	C2F-TCN [47]	-	-	-	-	-	42.6	37.5	25.3	35.2	53.4	-	-	-	-	-	-
	[47] ICC	2022	✓	✓	✓	C2F-TCN [47]	✓	60.2	53.5	35.6	56.6	65.3	52.9	49.0	36.6	45.6	61.3	77.9	71.6	54.6	71.4	68.2
10%	[48] SemiTAS	2022	-	-	-	MS-TCN [14]	-	56.9	51.3	39.0	57.7	49.5	47.3	42.7	31.8	43.6	58.0	71.5	66.0	52.9	67.2	62.6
	[47] ICC	2022	✓	✓	✓	C2F-TCN [47]	✓	64.6	59.0	42.2	61.9	68.8	67.3	64.9	49.2	56.9	68.6	83.7	81.9	66.6	76.4	73.3

segments and classification the action sequences as valid and invalid. It also alternates between HMM training and identifying these latent actions.

9.3 Single-Stage Learning

Previous works consists of an embedding step in which a joint space is learned using visual and/or temporal information and a clustering stage applied to the embedded features. Another type of work involves segmentation in a single stage. Aakur *et. al.* [60] present a self-supervised approach for detecting action boundaries using a single pass of the data. Their model, LSTM+AL, predicts the next frame’s feature and computes the difference between the predicted and observed features to define action boundaries.

UDE [132] is proposed to jointly learn embedding and clustering. Combining visual and positional encoding, they employ contrastive learning for clustering the latent space. Kumar *et. al.* [133] also combine representation learning and clustering into a single framework called TOT. They employ a mix of temporal optimal transport to preserve the temporal order of actions and a temporal coherence loss to retain the affinity across neighboring frames.

Recent work, TW-FINCH [53], captures the spatiotemporal similarities between frames and applies a temporally weighted hierarchical clustering algorithm to group semantically coherent video frames. This method does not require training because it is directly performed on the pre-computed features determine action boundaries. Similarly, ABD [54] identifies as action boundaries the abrupt change points along the similarity chain calculated between consecutive features.

10 SEMI-SUPERVISED APPROACHES

Compared to weak supervision that requires annotation for *every* training video, semi-supervised only requires dense labeling for a small *subset* of them. Ding and Yao [48] demonstrate that a small subset of dense annotations provides more information than single-frame supervision on the entire dataset. They claim that such supervision gives not only action information but also valuable action-level priors to guide the learning of the unlabeled videos. Their approach, SemiTAS [48], presents two novel loss functions for semi-supervised TAS, *i.e.*, action affinity loss and action continuity loss. Specifically, the affinity loss imposes the action composition and distribution prior by minimizing the KLD between closest label-unlabeled video pairs.

Likewise, ICC [47] proposes a semi-supervised method for TAS. ICC first learn a new set of feature representations with contrastive learning in a unsupervised way.

These features are later used to train a classifier for the semi-supervised setting. The network predictions are used as pseudo-labels to supervised unlabeled videos. With 40% labeled data, ICC performs comparably to the fully-supervised counterparts. We provide detailed performance comparisons in Tab. 10.

11 CONCLUSIONS AND OUTLOOK

This survey provided an overview of the techniques utilized in TAS, followed by a full literature evaluation as of the time of writing. The enormous quantity of literature demonstrates the subject’s expanding attention. Despite the rapid growth of the area, there are still a number of unexplored areas that we invite the community to examine.

Input Features. The mainstream works on TAS take visual feature vectors, either hand-crafted (IDT) [64] or extracted from an off-the-shelf CNN backbone (I3D) [66], as input for each frame. Using pre-computed features as inputs serves as a conventional practice for several other tasks as well, including temporal action localization, action anticipation, as it greatly reduces the computational demands and advocates a dedicated comparison of architectures, removing the impact of enhanced feature representations.

Nonetheless, as pointed out by [74], [75], pre-computed characteristics may favor static cues, *e.g.*, scene components, in frames. No empirical work to our knowledge has compared pre-computed features to training from raw images end-to-end, as training efficiency and GPU memory requirements are quite demanding.

Segment-Level Modeling. As mentioned in Section 6.2, the vast majority of current methods for the sequential modeling of actions are iterative and independent of feature learning. In addition, sequential modeling approaches are heavily utilized to post-process and refine the per-frame outputs. Exploring how to add sequence-related losses, such as edit scores that penalize segment-wise mistakes, into the learning process is also an interesting but under-explored direction. Segment-level loss readily coincides with the first interpretation of the TAS task (Eq. (1)). While the majority of existing techniques take a frame-wise prediction stance (Eq. (2)). We recommend a greater emphasis on solving the task at the segment level.

Forms of Supervision. Procedural video sequences feature enormous temporal redundancy in the supervisory signals. Temporal redundancy is due to the significant similarity between successive video frames of the same motion. Such redundancy has been proven by the comparable performance of using single-frame supervision vs.

fully-supervised setting [50], [126]. Yet, even single-frame supervision necessitates that a vigilant annotator skims over every video to verify that no activities are missed. Briefly explored in [50], how to handle missing actions in annotations could be a direction for TAS.

An additional component of supervision to consider is the inherent uncertainty of the action boundaries, as actions occurring in time are frequently not as distinct as an object in space. According to [48], these uncertainties in action boundaries can have a significant impact on model performance. It is therefore worthwhile to investigate how to define/label action boundaries.

Downstream tasks Outputs from temporal segmentation could be utilized in downstream tasks. For instance, [139] segments video streams in order to send alerts regarding missed actions. While [140] uses segmentation as a preliminary job for estimating the remaining time in lengthy surgery videos. Similarly, many approaches in action anticipation use segmentation techniques to represent prior observations with action labels [141], [142], [143]. This is because such labels contain high-level semantic information, which is preferred over visual characteristics for anticipation tasks [86]. An intelligent system that has acquired high-level semantic results via a TAS approach can summarize the contents of a movie, *i.e.*, video summarization [144].

Moreover, transferring the TAS to an online environment could make these strategies more useful to real-world applications. The initial attempts to achieve this objective were in [54], [145]. Yet, both approaches rely on frame-wise pre-computed features. The online segmentation of videos with end-to-end models could be a future trend.

In conclusion, TAS is a promising and rapidly evolving scientific topic with numerous potential real-world applications. In this survey, we present a detailed taxonomy of the problem, a systematic analysis of the fundamental methodologies, and a curated collection of current works classified by levels of supervision. We also highlight the chances and obstacles that lie ahead. We believe that this survey will provide an exposition of the topic and promote the growth of the community.

REFERENCES

- [1] S. Minaee, Y. Y. Boykov, F. Porikli, A. J. Plaza, N. Kehtarnavaz, and D. Terzopoulos, "Image segmentation using deep learning: A survey," *TPAMI*, 2022.
- [2] C. Feichtenhofer, H. Fan, J. Malik, and K. He, "Slowfast networks for video recognition," in *ICCV*, 2019.
- [3] J. Lin, C. Gan, and S. Han, "Tsm: Temporal shift module for efficient video understanding," in *ICCV*, 2019.
- [4] M. Patrick, D. Campbell, Y. Asano, I. Misra, F. Metze, C. Feichtenhofer, A. Vedaldi, and J. F. Henriques, "Keeping your eye on the ball: Trajectory attention in video transformers," *NeurIPS*, 2021.
- [5] H.-B. Zhang, Y.-X. Zhang, B. Zhong, Q. Lei, L. Yang, J.-X. Du, and D.-S. Chen, "A comprehensive survey of vision-based human action recognition methods," *Sensors*, vol. 19, no. 5, p. 1005, 2019.
- [6] Y. Kong and Y. Fu, "Human action recognition and prediction: A survey," *IJCV*, vol. 130, no. 5, pp. 1366–1401, 2022.
- [7] H. Xia and Y. Zhan, "A survey on temporal action localization," *IEEE Access*, vol. 8, 2020.
- [8] A. Baraka and M. H. Mohd Noor, "Weakly-supervised temporal action localization: a survey," *Neural Computing and Applications*, 2022.
- [9] N. P. Trong, H. Nguyen, K. Kazunori, and B. Le Hoai, "A comprehensive survey on human activity prediction," in *International Conference on Computational Science and Its Applications*. Springer, 2017, pp. 411–425.
- [10] A. Rasouli, "Deep learning for vision-based prediction: A survey," *arXiv preprint arXiv:2007.00095*, 2020.
- [11] L. Ding and C. Xu, "Tricronet: A hybrid temporal convolutional and recurrent network for video action segmentation," *arXiv preprint arXiv:1705.07818*, 2017.
- [12] A. Richard, H. Kuehne, A. Iqbal, and J. Gall, "Neuralnetwork-viterbi: A framework for weakly supervised video learning," in *CVPR*, 2018, pp. 7386–7395.
- [13] A. Richard, H. Kuehne, and J. Gall, "Action sets: Weakly supervised action segmentation without ordering constraints," in *CVPR*, 2018, pp. 5987–5996.
- [14] Y. A. Farha and J. Gall, "Ms-tcn: Multi-stage temporal convolutional network for action segmentation," in *CVPR*, 2019.
- [15] Z. Shou, D. Wang, and S.-F. Chang, "Temporal action localization in untrimmed videos via multi-stage cnns," in *CVPR*, 2016.
- [16] T. Lin, X. Liu, X. Li, E. Ding, and S. Wen, "Bmn: Boundary-matching network for temporal action proposal generation," in *ICCV*, 2019.
- [17] J. Barbić, A. Safonova, J.-Y. Pan, C. Faloutsos, J. K. Hodgins, and N. S. Pollard, "Segmenting motion capture data into distinct behaviors," in *Proceedings of Graphics Interface*, 2004.
- [18] F. Zhou, F. De la Torre, and J. K. Hodgins, "Aligned cluster analysis for temporal segmentation of human motion," in *2008 8th IEEE international conference on automatic face & gesture recognition*. IEEE, 2008, pp. 1–7.
- [19] —, "Hierarchical aligned cluster analysis for temporal clustering of human motion," *TPAMI*, vol. 35, no. 3, pp. 582–596, 2012.
- [20] S. Venkatesh, D. Moffat, and E. R. Miranda, "Investigating the effects of training set synthesis for audio segmentation of radio broadcast," *Electronics*, vol. 10, no. 7, p. 827, 2021.
- [21] E. B. Fox, M. C. Hughes, E. B. Sudderth, M. I. Jordan *et al.*, "Joint modeling of multiple time series via the beta process with application to motion capture segmentation," *The Annals of Applied Statistics*, vol. 8, no. 3, pp. 1281–1313, 2014.
- [22] D. Zhukov, J.-B. Alayrac, R. G. Cinbis, D. Fouhey, I. Laptev, and J. Sivic, "Cross-task weakly supervised learning from instructional videos," in *CVPR*, 2019.
- [23] K. Zhang, W.-L. Chao, F. Sha, and K. Grauman, "Video summarization with long short-term memory," in *ECCV*, 2016.
- [24] E. Elhamifar and D. Huynh, "Self-supervised multi-task procedure learning from instructional videos," in *ECCV*, 2020.
- [25] Z. Naing and E. Elhamifar, "Procedure completion by learning from partial summaries," in *BMVC*, 2020.
- [26] A. Fathi, X. Ren, and J. M. Rehg, "Learning to recognize objects in egocentric activities," in *CVPR*, 2011.
- [27] S. Stein and S. J. McKenna, "Combining embedded accelerometers with computer vision for recognizing food preparation activities," in *UBICOMP*. ACM, 2013.
- [28] H. Kuehne, A. Arslan, and T. Serre, "The language of actions: Recovering the syntax and semantics of goal-directed human activities," in *CVPR*, 2014.
- [29] D. Damen, H. Doughty, G. M. Farinella, A. Furnari, E. Kazakos, J. Ma, D. Moltisanti, J. Munro, T. Perrett, W. Price *et al.*, "Rescaling egocentric vision: collection, pipeline and challenges for epic-kitchens-100," *IJCV*, vol. 130, no. 1, pp. 33–55, 2022.
- [30] Y. Ben-Shabat, X. Yu, F. Saleh, D. Campbell, C. Rodriguez-Opazo, H. Li, and S. Gould, "The ikea asm dataset: Understanding people assembling furniture through actions, objects and pose," in *WACV*, 2021.
- [31] F. Ragusa, A. Furnari, S. Livatino, and G. M. Farinella, "The meccano dataset: Understanding human-object interactions from egocentric videos in an industrial-like domain," in *WACV*, 2021.
- [32] F. Sener, D. Chatterjee, D. Sheleporov, K. He, D. Singhania, R. Wang, and A. Yao, "Assembly101: A large-scale multi-view video dataset for understanding procedural activities," in *CVPR*, 2022.
- [33] G. Cicirelli, R. Marani, L. Romeo, M. G. Domínguez, J. Heras, A. G. Perri, and T. D'Orazio, "The ha4m dataset: Multi-modal monitoring of an assembly task for human action recognition in manufacturing," *Scientific Data*, vol. 9, no. 1, p. 745, 2022.
- [34] J.-B. Alayrac, P. Bojanowski, N. Agrawal, J. Sivic, I. Laptev, and S. Lacoste-Julien, "Unsupervised learning from narrated instructional videos," in *CVPR*, 2016.
- [35] L. Zhou, C. Xu, and J. J. Corso, "Towards automatic learning of procedures from web instructional videos," in *AAAI*, 2018.
- [36] Y. Tang, D. Ding, Y. Rao, Y. Zheng, D. Zhang, L. Zhao, J. Lu, and J. Zhou, "Coin: A large-scale dataset for comprehensive instructional video analysis," in *CVPR*, 2019, pp. 1207–1216.

[37] N. Hussein, E. Gavves, and A. W. Smeulders, "Timeception for complex action recognition," in *CVPR*, 2019, pp. 254–263.

[38] —, "Pic: Permutation invariant convolution for recognizing long-range activities," *arXiv preprint arXiv:2003.08275*, 2020.

[39] M. Z. Shou, S. W. Lei, W. Wang, D. Ghadiyaram, and M. Feiszli, "Generic event boundary detection: A benchmark for event segmentation," in *ICCV*, 2021.

[40] D. Damen, H. Doughty, G. M. Farinella, S. Fidler, A. Furnari, E. Kazakos, D. Moltisanti, J. Munro, T. Perrett, W. Price, and M. Wray, "Scaling egocentric vision: The epic-kitchens dataset," in *ECCV*, 2018.

[41] Y. Li, M. Liu, and J. M. Rehg, "In the eye of beholder: Joint learning of gaze and actions in first person video," in *ECCV*, 2018, pp. 619–635.

[42] J. Malmaud, J. Huang, V. Rathod, N. Johnston, A. Rabinovich, and K. Murphy, "What's cookin'? interpreting cooking videos using text, speech and vision," in *NAACL*, 2015.

[43] F. Sener and A. Yao, "Zero-shot anticipation for instructional activities," in *ICCV*, 2019, pp. 862–871.

[44] Z. Liu, Z. Miao, X. Zhan, J. Wang, B. Gong, and S. X. Yu, "Large-scale long-tailed recognition in an open world," in *CVPR*, 2019.

[45] B. Kang, S. Xie, M. Rohrbach, Z. Yan, A. Gordo, J. Feng, and Y. Kalantidis, "Decoupling representation and classifier for long-tailed recognition," *arXiv preprint arXiv:1910.09217*, 2019.

[46] C. Lea, M. D. Flynn, R. Vidal, A. Reiter, and G. D. Hager, "Temporal convolutional networks for action segmentation and detection," in *CVPR*, 2017, pp. 156–165.

[47] D. Singhania, R. Rahaman, and A. Yao, "Iterative contrast-classify for semi-supervised temporal action segmentation," in *AAAI*, vol. 36, no. 2, 2022.

[48] G. Ding and A. Yao, "Leveraging action affinity and continuity for semi-supervised temporal action segmentation," in *ECCV*, 2022.

[49] J. Li and S. Todorovic, "Action shuffle alternating learning for unsupervised action segmentation," in *CVPR*, 2021.

[50] R. Rahaman, D. Singhania, A. Thiery, and A. Yao, "A generalized & robust framework for timestamp supervision in temporal action segmentation," in *ECCV*, 2022.

[51] G. Ding and A. Yao, "Temporal action segmentation with high-level complex activity labels," *TMM*, 2022.

[52] F. Sener and A. Yao, "Unsupervised learning and segmentation of complex activities from video," in *CVPR*, 2018, pp. 8368–8376.

[53] S. Sarfraz, N. Murray, V. Sharma, A. Diba, L. Van Gool, and R. Stiefelhagen, "Temporally-weighted hierarchical clustering for unsupervised action segmentation," in *CVPR*, 2021.

[54] Z. Du, X. Wang, G. Zhou, and Q. Wang, "Fast and unsupervised action boundary detection for action segmentation," in *CVPR*, 2022.

[55] C. Lea, A. Reiter, R. Vidal, and G. D. Hager, "Segmental spatiotemporal cnns for fine-grained action segmentation," in *ECCV*. Springer, 2016, pp. 36–52.

[56] J. Li and S. Todorovic, "Set-constrained viterbi for set-supervised action segmentation," in *CVPR*, 2020, pp. 10820–10829.

[57] H. W. Kuhn, "The hungarian method for the assignment problem," *Naval research logistics quarterly*, vol. 2, no. 1-2, 1955.

[58] T. Li and C. Ding, "The relationships among various nonnegative matrix factorization methods for clustering," in *ICDM*, 2006.

[59] J. Chang, Y. Guo, L. Wang, G. Meng, S. Xiang, and C. Pan, "Deep discriminative clustering analysis," *arXiv preprint arXiv:1905.01681*, 2019.

[60] S. N. Aakur and S. Sarkar, "A perceptual prediction framework for self supervised event segmentation," in *CVPR*, 2019.

[61] A. Kukleva, H. Kuehne, F. Sener, and J. Gall, "Unsupervised learning of action classes with continuous temporal embedding," in *CVPR*, 2019.

[62] R. G. VidalMata, W. J. Scheirer, A. Kukleva, D. Cox, and H. Kuehne, "Joint visual-temporal embedding for unsupervised learning of actions in untrimmed sequences," in *WACV*, 2021.

[63] H. Wang, A. Kläser, C. Schmid, and C.-L. Liu, "Action recognition by dense trajectories," in *CVPR*. IEEE, 2011.

[64] H. Wang and C. Schmid, "Action recognition with improved trajectories," in *ICCV*, 2013.

[65] F. Perronnin, J. Sánchez, and T. Mensink, "Improving the fisher kernel for large-scale image classification," in *ICCV*, 2010.

[66] J. Carreira and A. Zisserman, "Quo vadis, action recognition? a new model and the kinetics dataset," in *CVPR*, 2017.

[67] S. Ioffe and C. Szegedy, "Batch normalization: Accelerating deep network training by reducing internal covariate shift," in *ICML*. PMLR, 2015, pp. 448–456.

[68] W. Kay, J. Carreira, K. Simonyan, B. Zhang, C. Hillier, S. Vijayanarasimhan, F. Viola, T. Green, T. Back, P. Natsev *et al.*, "The kinetics human action video dataset," *arXiv preprint arXiv:1705.06950*, 2017.

[69] C. Zach, T. Pock, and H. Bischof, "A duality based approach for realtime tv-l 1 optical flow," in *Joint pattern recognition symposium*. Springer, 2007.

[70] A. Richard, "Temporal segmentation of human actions in videos," Ph.D. dissertation, Universitäts-und Landesbibliothek Bonn, 2019.

[71] T. Chen, S. Kornblith, M. Norouzi, and G. Hinton, "A simple framework for contrastive learning of visual representations," in *ICML*. PMLR, 2020.

[72] R. Qian, T. Meng, B. Gong, M.-H. Yang, H. Wang, S. Belongie, and Y. Cui, "Spatiotemporal contrastive video representation learning," in *CVPR*, 2021.

[73] G. Lorre, J. Rabarisoa, A. Orcesi, S. Ainouz, and S. Canu, "Temporal contrastive pretraining for video action recognition," in *WACV*, 2020.

[74] J. Choi, C. Gao, J. C. Messou, and J.-B. Huang, "Why can't i dance in the mall? learning to mitigate scene bias in action recognition," in *NeurIPS*, 2019.

[75] D.-A. Huang, V. Ramanathan, D. Mahajan, L. Torresani, M. Paluri, L. Fei-Fei, and J. Carlos Niebles, "What makes a video a video: Analyzing temporal information in video understanding models and datasets," in *CVPR*, 2018.

[76] Y. Li and N. Vasconcelos, "Repair: Removing representation bias by dataset resampling," in *CVPR*, 2019, pp. 9572–9581.

[77] Y. Li, Y. Li, and N. Vasconcelos, "Resound: Towards action recognition without representation bias," in *ECCV*, 2018.

[78] K. Cho, B. van Merriënboer, C. Gulcehre, D. Bahdanau, F. Bougares, H. Schwenk, and Y. Bengio, "Learning phrase representations using rnn encoder–decoder for statistical machine translation," in *EMNLP*, 2014.

[79] A. Richard, H. Kuehne, and J. Gall, "Weakly supervised action learning with rnn based fine-to-coarse modeling," in *CVPR*, 2017.

[80] Y. Huang, Y. Sugano, and Y. Sato, "Improving action segmentation via graph-based temporal reasoning," in *CVPR*, 2020.

[81] L. Ding and C. Xu, "Weakly-supervised action segmentation with iterative soft boundary assignment," in *CVPR*, 2018.

[82] P. Lei and S. Todorovic, "Temporal deformable residual networks for action segmentation in videos," in *CVPR*, 2018, pp. 6742–6751.

[83] D. Singhania, R. Rahaman, and A. Yao, "Coarse to fine multi-resolution temporal convolutional network," *arXiv preprint arXiv:2105.10859*, 2021.

[84] O. Ronneberger, P. Fischer, and T. Brox, "U-net: Convolutional networks for biomedical image segmentation," in *International Conference on Medical image computing and computer-assisted intervention*. Springer, 2015.

[85] S.-J. Li, Y. AbuFarha, Y. Liu, M.-M. Cheng, and J. Gall, "Mstcn++: Multi-stage temporal convolutional network for action segmentation," *TPAMI*, 2020.

[86] F. Sener, D. Singhania, and A. Yao, "Temporal aggregate representations for long-range video understanding," in *ECCV*, 2020.

[87] Y. Tang, X. Zhang, L. Ma, J. Wang, S. Chen, and Y.-G. Jiang, "Non-local netvlad encoding for video classification," in *ECCV*, 2018.

[88] F. Yi, H. Wen, and T. Jiang, "Asformer: Transformer for action segmentation," in *BMVC*, 2021.

[89] N. Behrmann, S. A. Golestaneh, Z. Kolter, J. Gall, and M. Noroozi, "Unified fully and timestamp supervised temporal action segmentation via sequence to sequence translation," in *ECCV*, 2022.

[90] X. Zhu, W. Su, L. Lu, B. Li, X. Wang, and J. Dai, "Deformable detr: Deformable transformers for end-to-end object detection," *arXiv preprint arXiv:2010.04159*, 2020.

[91] M. J. Powell, "A direct search optimization method that models the objective and constraint functions by linear interpolation," in *Advances in optimization and numerical analysis*. Springer, 1994.

[92] A. Viterbi, "Error bounds for convolutional codes and an asymptotically optimum decoding algorithm," *IEEE Transactions on Information Theory*, vol. 13, no. 2, pp. 260–269, 1967.

[93] Y. Souri, Y. A. Farha, F. Despinoy, G. Francesca, and J. Gall, "Fifa: Fast inference approximation for action segmentation," in *GCPR*, 2021.

[94] D. Moltisanti, S. Fidler, and D. Damen, "Action recognition from single timestamp supervision in untrimmed videos," in *CVPR*, 2019.

[95] Z. Wang, Z. Gao, L. Wang, Z. Li, and G. Wu, "Boundary-aware cascade networks for temporal action segmentation," in *ECCV*, 2020.

[96] Y. Ishikawa, S. Kasai, Y. Aoki, and H. Kataoka, "Alleviating over-segmentation errors by detecting action boundaries," in *WACV*, 2021.

[97] B. Singh, T. K. Marks, M. Jones, O. Tuzel, and M. Shao, "A multi-stream bi-directional recurrent neural network for fine-grained action detection," in *CVPR*, 2016, pp. 1961–1970.

[98] K.-N. C. Mac, D. Joshi, R. A. Yeh, J. Xiong, R. S. Feris, and M. N. Do, "Learning motion in feature space: Locally-consistent deformable convolution networks for fine-grained action detection," in *ICCV*, 2019, pp. 6282–6291.

[99] H. Gammulle, T. Fernando, S. Denman, S. Sridharan, and C. Fookes, "Coupled generative adversarial network for continuous fine-grained action segmentation," in *WACV*, 2019.

[100] H. Kuehne, J. Gall, and T. Serre, "An end-to-end generative framework for video segmentation and recognition," in *WACV*. IEEE, 2016, pp. 1–8.

[101] Y. Zhang, K. Muandet, Q. Ma, H. Neumann, and S. Tang, "Frontal low-rank random tensors for fine-grained action segmentation," *arXiv preprint arXiv:1906.01004*, 2019.

[102] D. Wang, Y. Yuan, and Q. Wang, "Gated forward refinement network for action segmentation," *Neurocomputing*, vol. 407, 2020.

[103] M.-H. Chen, B. Li, Y. Bao, and G. AlRegib, "Action segmentation with mixed temporal domain adaptation," in *WACV*, 2020.

[104] M.-H. Chen, B. Li, Y. Bao, G. AlRegib, and Z. Kira, "Action segmentation with joint self-supervised temporal domain adaptation," in *CVPR*, 2020, pp. 9454–9463.

[105] S.-H. Gao, Q. Han, Z.-Y. Li, P. Peng, L. Wang, and M.-M. Cheng, "Global2local: Efficient structure search for video action segmentation," in *CVPR*, 2021.

[106] S. Karaman, L. Seidenari, and A. Del Bimbo, "Fast saliency based pooling of fisher encoded dense trajectories," in *ECCV THUMOS Workshop*, vol. 1, no. 2, 2014, p. 5.

[107] M. Rohrbach, S. Amin, M. Andriluka, and B. Schiele, "A database for fine grained activity detection of cooking activities," in *CVPR*, 2012.

[108] Y. Cheng, Q. Fan, S. Pankanti, and A. Choudhary, "Temporal sequence modeling for video event detection," in *CVPR*, 2014.

[109] A. Fathi, A. Farhadi, and J. M. Rehg, "Understanding egocentric activities," in *ICCV*, 2011, pp. 407–414.

[110] A. Fathi and J. M. Rehg, "Modeling actions through state changes," in *CVPR*, 2013, pp. 2579–2586.

[111] N. N. Vo and A. F. Bobick, "From stochastic grammar to bayes network: Probabilistic parsing of complex activity," in *CVPR*, 2014, pp. 2641–2648.

[112] H. Pirsiavash and D. Ramanan, "Parsing videos of actions with segmental grammars," in *CVPR*, 2014.

[113] A. Richard and J. Gall, "Temporal action detection using a statistical language model," in *CVPR*, 2016.

[114] H. Kuehne, A. Richard, and J. Gall, "Weakly supervised learning of actions from transcripts," *CVIU*, vol. 163, pp. 78–89, 2017.

[115] P. Bojanowski, R. Lajugie, F. Bach, I. Laptev, J. Ponce, C. Schmid, and J. Sivic, "Weakly supervised action labeling in videos under ordering constraints," in *ECCV*, 2014.

[116] Z. Lu and E. Elhamifar, "Weakly-supervised action segmentation and alignment via transcript-aware union-of-subspaces learning," in *ICCV*, 2021.

[117] D. Huang, F. Li, and J. C. Niebles, "Connectionist temporal modeling for weakly supervised action labeling," in *ECCV*, 2016.

[118] A. Graves, S. Fernández, F. Gomez, and J. Schmidhuber, "Connectionist temporal classification: labelling unsegmented sequence data with recurrent neural networks," in *ICML*, 2006.

[119] C.-Y. Chang, D.-A. Huang, Y. Sui, L. Fei-Fei, and J. C. Niebles, "D3tw: Discriminative differentiable dynamic time warping for weakly supervised action alignment and segmentation," in *CVPR*, 2019, pp. 3546–3555.

[120] J. Li, P. Lei, and S. Todorovic, "Weakly supervised energy-based learning for action segmentation," in *ICCV*, 2019.

[121] Y. Souri, M. Fayyaz, L. Minciullo, G. Francesca, and J. Gall, "Fast weakly supervised action segmentation using mutual consistency," *TPAMI*, 2021.

[122] X. Chang, F. Tung, and G. Mori, "Learning discriminative prototypes with dynamic time warping," in *CVPR*, 2021.

[123] M. Fayyaz and J. Gall, "Sct: Set constrained temporal transformer for set supervised action segmentation," in *CVPR*, 2020.

[124] J. Li and S. Todorovic, "Anchor-constrained viterbi for set-supervised action segmentation," in *CVPR*, 2021.

[125] Z. Lu and E. Elhamifar, "Set-supervised action learning in procedural task videos via pairwise order consistency," in *CVPR*, 2022.

[126] Z. Li, Y. Abu Farha, and J. Gall, "Temporal action segmentation from timestamp supervision," in *CVPR*, 2021.

[127] M. A. Fligner and J. S. Verducci, "Distance based ranking models," *Journal of the Royal Statistical Society. Series B (Methodological)*, pp. 359–369, 1986.

[128] K. Goel and E. Brunskill, "Learning procedural abstractions and evaluating discrete latent temporal structure," in *ICLR*, 2019.

[129] Z. Wang, H. Chen, X. Li, C. Liu, Y. Xiong, J. Tighe, and C. Fowlkes, "Sscap: Self-supervised co-occurrence action parsing for unsupervised temporal action segmentation," in *WACV*, 2022.

[130] S. Benaim, A. Ephrat, O. Lang, I. Mosseri, W. T. Freeman, M. Rubinstein, M. Irani, and T. Dekel, "Speednet: Learning the speediness in videos," in *CVPR*, 2020.

[131] K. Simonyan and A. Zisserman, "Very deep convolutional networks for large-scale image recognition," *arXiv preprint arXiv:1409.1556*, 2014.

[132] S. Swetha, H. Kuehne, Y. S. Rawat, and M. Shah, "Unsupervised discriminative embedding for sub-action learning in complex activities," in *ICIP*. IEEE, 2021.

[133] S. Kumar, S. Haresh, A. Ahmed, A. Konin, M. Z. Zia, and Q.-H. Tran, "Unsupervised action segmentation by joint representation learning and online clustering," in *CVPR*, 2022.

[134] H. Khan, S. Haresh, A. Ahmed, S. Siddiqui, A. Konin, M. Z. Zia, and Q.-H. Tran, "Timestamp-supervised action segmentation with graph convolutional networks," in *IROS*, 2022.

[135] P. Bojanowski, R. Lajugie, E. Grave, F. Bach, I. Laptev, J. Ponce, and C. Schmid, "Weakly-supervised alignment of video with text," in *ICCV*, 2015, pp. 4462–4470.

[136] O. Sener, A. R. Zamir, S. Savarese, and A. Saxena, "Unsupervised semantic parsing of video collections," in *ICCV*, 2015.

[137] D. Fried, J.-B. Alayrac, P. Blunsom, C. Dyer, S. Clark, and A. Nematzadeh, "Learning to segment actions from observation and narration," in *ACL*, 2020.

[138] S. Bansal, C. Arora, and C. Jawahar, "My view is the best view: Procedure learning from egocentric videos," in *ECCV*, 2022.

[139] B. Soran, A. Farhadi, and L. Shapiro, "Generating notifications for missing actions: Don't forget to turn the lights off!" in *ICCV*, 2015, pp. 4669–4677.

[140] D. Rivoir, S. Bodenstedt, F. von Bechtolsheim, M. Distler, J. Weitz, and S. Speidel, "Unsupervised temporal video segmentation as an auxiliary task for predicting the remaining surgery duration," in *OR 2.0 Context-Aware Operating Theaters and Machine Learning in Clinical Neuroimaging*. Springer, 2019, pp. 29–37.

[141] Y. A. Farha, A. Richard, and J. Gall, "When will you do what? anticipating temporal occurrences of activities," in *CVPR*, 2018.

[142] Q. Ke, M. Fritz, and B. Schiele, "Time-conditioned action anticipation in one shot," in *CVPR*, 2019.

[143] H. Gammulle, S. Denman, S. Sridharan, and C. Fookes, "Forecasting future action sequences with neural memory networks," in *BMVC*, 2019.

[144] E. Apostolidis, E. Adamantidou, A. I. Metsai, V. Mezaris, and I. Patras, "Video summarization using deep neural networks: A survey," *Proceedings of the IEEE*, vol. 109, no. 11, 2021.

[145] R. Ghoddoosian, I. Dwivedi, N. Agarwal, C. Choi, and B. Darioush, "Weakly-supervised online action segmentation in multi-view instructional videos," in *CVPR*, 2022.